

1 A new comprehensive Eye-Tracking Test 2 Battery concurrently evaluating the Pupil 3 Labs Glasses and the EyeLink 1000

4 **Benedikt V. Ehinger^{1,2}, Katharina Groß¹, Inga Ibs¹, and Peter König^{1,3}**

5 ¹**Institute of Cognitive Science, Osnabrück University**

6 ²**Donders Institute for Brain, Cognition and Behaviour, Radboud University**

7 ³**Department of Neurophysiology and Pathophysiology, University Medical Center
8 Hamburg-Eppendorf**

9 Corresponding author:

10 Benedikt V. Ehinger¹

11 Email address: b.ehinger@donders.ru.nl

12 ABSTRACT

13 Eye-tracking experiments rely heavily on good data quality of eye-trackers. Unfortunately, it is often
14 that only the spatial accuracy and precision values are available from the manufacturers. These two
15 values alone are not sufficient enough to serve as a benchmark for an eye-tracker: Eye-tracking quality
16 deteriorates during an experimental session due to head movements, changing illumination or calibration
17 decay. Additionally, different experimental paradigms require the analysis of different types of eye
18 movements, for instance smooth pursuit movements, blinks or microsaccades, which themselves cannot
19 readily be evaluated by using spatial accuracy or precision alone. To obtain a more comprehensive
20 description of properties, we developed an extensive eye-tracking test battery. In 10 different tasks, we
21 evaluated eye-tracking related measures such as: the decay of accuracy, fixation durations, pupil dilation,
22 smooth pursuit movement, microsaccade detection, blink detection, or the influence of head motion.
23 For some measures, true theoretical values exist. For others, a relative comparison to a gold standard
24 eye-tracker is needed. Therefore, we collected our gaze data simultaneously from a gold standard remote
25 EyeLink 1000 eye-tracker and compared it with the mobile Pupil Labs glasses.
26 As expected, the average spatial accuracy of 0.57° for the EyeLink 1000 eye-tracker was better than the
27 0.82° for the Pupil Labs glasses (N=15). Furthermore, we detected less fixations and shorter saccade
28 durations for the Pupil Labs glasses. Similarly, we found fewer microsaccades using the Pupil Labs
29 glasses. The accuracy over time decayed only slightly for the EyeLink 1000, but strongly for the Pupil
30 Labs glasses. Finally we observed that the measured pupil diameters differed between eye-trackers on
31 the individual subject level but not the group level.
32 To conclude, our eye-tracking test battery offers 10 tasks that allow us to benchmark the many parameters
33 of interest in stereotypical eye-tracking situations, or addresses a common source of confounds in
34 measurement errors (e.g. yaw and roll head movements).
35 All recorded eye-tracking data (including Pupil Labs' eye video files), the stimulus code for the test battery
36 and the modular analysis pipeline are available (<https://github.com/behinger/etcomp>).

37 **BVE, KG, II and PK** conceived the experiment. **II** and **BVE** created the experiment and recorded the
38 gaze data. **BVE** and **KG** performed the analysis. **BVE, KG** and **PK** reviewed the manuscript critically.

39 1 INTRODUCTION

40 Eye-tracking has become a common method in cognitive neuroscience and is increasingly utilized by
41 diagnostic medicine, performance monitoring, or consumer experience research (Duchowski, 2007;
42 Holmqvist et al., 2011; Liversedge et al., 2012). These applications are diverse, make use of many
43 different eye movement parameters, and have different technical requirements. Thus, a single index will
44 not be sufficient to characterize the suitability of an eye-tracker for a specific application, but a more
45 comprehensive test is needed.

46 In the following, we will shortly highlight several of these applications, their eye movement parameters
47 and technical challenges:

48 Eye-tracking offers promising insights into diagnostics of clinical populations but patients often have
49 a limited attentional span and motor deficits make eye-tracking much more difficult (Açık et al., 2010;
50 Dowiasch et al., 2015; Cludius et al., 2017; Fischer et al., 2016). In other studies, smallest eye movements
51 (microsaccades) are of interest as they can reveal small attentional effects (Rolfs, 2009) or even confound
52 fMRI effects (Mostert et al., 2018) and EEG analyses (Yuval-Greenberg et al., 2008). Mobile eye-tracking
53 studies show the importance of enactive paradigms (Marius 't Hart et al., 2009; Einhäuser and König,
54 2010) which are always accompanied by smooth pursuit and head movements; a field of investigation
55 in itself (Einhäuser et al., 2007, 2009; Schumann et al., 2008). A different but very interesting eye
56 behavior is blinks which can be related to dopamine levels (Riggs et al., 1981; but see Sescousse et al.,
57 2018 for recent more nuanced evidence), saccadic suppression (Burr, 2005), or time perception (Terhune
58 et al., 2016). Further, in combination with physiological recordings, for instance EEG (Dimigen
59 et al., 2011; Plöchl et al., 2012; Ehinger et al., 2015), fMRI (Bonhage et al., 2015a; Petit et al., 1997;
60 Bonhage et al., 2015b), or skin conductance (Wieser et al., 2009), eye-tracking allows to investigate more
61 complex and realistic behavioral paradigms and ultimately generate new insights into brain function
62 and dysfunction (Eckstein et al., 2017). Another field of application is pupil dilation, a physiological
63 measure with many cognitive applications (Mathôt, 2018): It allows to track attention (Wahn et al., 2016),
64 investigate decision making (Urai et al., 2018), and even communicate with locked-in syndrome patients
65 (Stoll et al., 2013). These examples illustrate the diversity of eye-tracking paradigms but nevertheless can
66 only show a fraction of all possible applications.

67 It is clear that such a range of paradigms requires that each eye movement needs to be characterized by
68 its own quality measure (e.g. pupil dilation accuracy, smooth pursuit and blink detectability or calibration
69 decay due to head movements). Here, we argue that the characterization of an eye-tracker requires a large
70 set of experimental tasks eliciting different eye movement types in a controlled manner.

71 Estimating the performance of an eye-tracker is difficult, because many eye-tracking measures cannot
72 be compared to a theoretical true value. For instance, standard calibration methods rely on participants
73 fixating given visual stimuli, typically dots. However, even when participants think they fixate on a
74 dot, their actual gaze point will never be perfectly resting on the dot. Unknown to them, miniature eye
75 movements like drift and microsaccades move the gaze point around the fixation target (Rolfs, 2009). To
76 nevertheless estimate the reliability of a single eye-tracker and compensate for the lack of ground truth at
77 the same time, it is necessary to measure the participants' gaze with two eye-trackers simultaneously: a
78 gold standard eye-tracker and the target eye-tracker.

79 Consequently, we recorded the participants' gaze with two video-based eye-trackers at the same time:
80 the stationary EyeLink 1000 (SR research) and the mobile Pupil Labs glasses (Pupil Labs, Berlin). The
81 EyeLink 1000 is a popular high-end remote eye-tracker which we use as our "gold standard" reference.
82 It is a video based eye-tracker with one of the best accuracy and precision (Holmqvist, 2017) currently
83 available. We chose to benchmark the mobile Pupil Labs eye-tracking glasses because they are special
84 in several regards: For mobile eye-tracking glasses, they offer high sampling rates (current versions
85 200 Hz per eye, our version up to 120 Hz per eye), along with open source hardware and software, and
86 the eye-tracker is quite affordable. Depending on the specifications of the two eye-trackers, the price can
87 vary by a factor of 15. These features foster the wide usage of this mobile eye-tracker and motivate the
88 comparison to the gold standard.

89 There is little published data on the performance of eye-trackers and even less that is published
90 independently from the manufacturers. Worse, no standards to measure and report eye-tracker performance
91 exist (Holmqvist et al., 2012) and open source systematic benchmarks for eye-tracking devices are not
92 available. However, as we have seen, the problem is complex, as single measures like the popular spatial
93 accuracy and precision, even though they are arguably two of the most useful single metrics, will never be
94 able to fully describe the performance of an eye-tracker.

95 For these reasons, we developed a new paradigm to evaluate the data quality of the most common
96 eye-tracking related parameters. Our test battery consists of: fixation and saccade properties in an artificial
97 grid and in a free-viewing task, decay of accuracy, smooth pursuit, pupil dilation, microsaccades, blink
98 detection, and the influence of head motion.

99 To circumvent the need for theoretical true values, we make use of relative comparisons between
100 two simultaneously recorded eye-trackers. Our large set of analyzed eye-tracking parameters offers a

101 comprehensive characterization of the tested eye-trackers.

102 In order to make our analyses in this paper reproducible and to offer a dataset for benchmarking
103 purposes, we made the recorded data (including the eye camera video streams) available on figshare
104 (10.6084/m9.figshare.c.4379810). The source code of the eye-tracking test battery and the
105 modular analysis pipeline are available on GitHub (<https://github.com/behinger/etcomp>¹).

106 **2 METHODS**

107 **2.1 Methods of Data Acquisition**

108 **2.1.1 Participants**

109 We recruited 15 participants (mean age 24, range 19 to 28, 9 female, 0 left-handed, 3 left-dominant
110 eye) at Osnabrück University. Eligibility criteria were: no glasses, no drug use, no photosensitive
111 migraine or epilepsy, and more than 5 hours of sleep the last night before the experiment. 11 additional
112 participants were excluded from the analysis: 6 due to exceeding pre-specified calibration accuracy limits
113 (2 Pupil Labs glasses, 3 EyeLink 1000 and 1 both eye-trackers), and 5 due to software failures (see
114 Section 1). Prior to the experiment, we used a calibrated online LogMar chart test (Open Optometry
115 (2018), www.openoptometry.com) to ensure a visual acuity below 6/6 using a single test line with
116 5 letters. Ocular dominance was detected with the “hole-in-card” test by using the participants’ hands
117 and centered gaze. After the experiment, we collected information about the participants’ age, gender,
118 handedness, and eye color. We compensated the participants with either EUR 9 or one course credit
119 per hour. The participants gave written consent and the study was approved by the ethic committee of
120 Osnabrück University (4/71043.5).

121 **2.1.2 Experimental Setup and Recording Devices**

122 The experiment was conducted at the Institute of Cognitive Science at Osnabrück University. In a
123 separated recording room, we used a 24” monitor (XL2420T, BenQ) with 1920×1080 pixels resolution
124 and a 120 Hz refresh rate. The effective area of the monitor was 1698×758 pixels because we displayed
16 visual markers for the Pupil Labs eye-tracker in the margins of the monitor (see Figure 1). A single



125 **Figure 1.** The remote eye-tracker EyeLink 1000 is located beneath the computer screen that displays the
126 stimuli. The participant wears the mobile Pupil Labs glasses. The auxiliary calibration monitor on the left
127 was turned off during the experiment. (Subject’s consent to publish this image was granted)

125 USB-loudspeaker was used to produce a beep sound for the auditory stimuli. The participants were seated
126

¹ Archived version: <https://doi.org/10.5281/zenodo.2553447>

127 at a distance of 60 cm to the monitor and the chamber light was kept on. We measured 52 cd/m² from the
128 point of view of the subject facing the monitor with the average grey luminance.

129 The participants' eye movements were recorded simultaneously by one stationary and one mobile
130 eye-tracking device. A desktop mounted eye-tracker (EyeLink 1000, SR-Research Ltd., Mississauga,
131 Ontario, Canada) was used to make monocular recordings of the participants' dominant eye (500 Hz,
132 head free-to-move mode). Concurrently, a mobile eye-tracker (Pupil Labs glasses, Pupil Labs, Berlin,
133 Germany) was used to make binocular recordings of the participants' eyes (Figure 1). The Pupil Labs
134 glasses have three cameras: one world camera (1920 × 1080 pixels, 100° fisheye field of view, 60 Hz
135 sampling frequency on a subset of 1280 × 720 pixels) to record the participant's view and one eye-camera
136 for each eye (1920 × 1080 pixels, 120 Hz sampling frequency on a subset of 320 × 280 pixels). We
137 recorded eye movements using Pupil Labs' capture release 1.65 (November 2017).

138 We conducted the experiment using three computers: One stimulus computer and two recording
139 computers, one for each eye-tracking device. To temporally align the recordings, we used concurrent
140 trigger signals via Ethernet at all experimental events. For the EyeLink 1000 we used the EyeLink Toolbox
141 (Cornelissen et al., 2002), for the Pupil Labs glasses we used zeroMQ packages (Wilmet, 2017). In
142 separate measurements, we estimated round trip delay times with both recording computers of below
143 1 ms.

144 The experiment script was written in Matlab (R2016b, Mathworks) using the Psychophysics Toolbox 3
145 Brainard (1997); Pelli (1997); Kleiner et al. (2007), Eyelink Toolbox (Cornelissen et al., 2002) and custom
146 scripts based on the ZMQ protocol for communication with the Pupil Labs Glasses. The analyses
147 were conducted using Python 3.5.2 (van Rossum, 1995) with a version of Pupil Labs from April 2018
148 (git version: f32ef8e), pyEDFread (Wilming, 2015) , NumPy (Oliphant, 2006), pandas (McKinney,
149 2010), and SciPy (Jones et al., 2001). For visualization, we used plotnine (Kibirige et al., 2018) and
150 Matplotlib (Hunter, 2007).

151 **2.1.3 Experimental Design**

152 All participants were recorded by a single, newly trained experimenter (Author Inga Ibs <1 year experience)
153 under the supervision of an experienced experimenter (Author Benedikt V. Ehinger >5 years
154 experience).

155 The experiment lasted approximately 60 min. The session started with a brief oral explanation of
156 the upcoming tasks, then we obtained written consent and an anamnesis questionnaire, which was used
157 to exclude participants who suffer from a photosensitive migraine or epilepsy. We then identified their
158 dominant eye and checked their acuity (see Section 2.1.1 for procedures). Before the experiment, the
159 experimenter emphasized the importance to look at the fixation targets.

160 The experiment consisted of 6 repetitions (blocks) of a set of 10 tasks (Figure 2). Each block had the
161 same order of tasks (see below). Participants read a written instruction prior to each task ² and saw a
162 green fixation target at the center of the monitor. Participants then started the tasks in their own time by
163 pressing the space bar. In order to examine a variety of properties of the eye-trackers, each task either
164 measures attributes of the eye-tracking devices (e.g. accuracy), estimates suitability for specialist studies
165 (e.g. pupil diameter and microsaccades), depicts a stereotypical eye-tracking situation (e.g. free viewing),
166 or addresses aspects of more complex behavioural situations including head movements (e.g. yaw and
167 roll head movements) and dynamic stimuli (e.g. smooth pursuit). An overview of the tasks and stimuli is
168 given in Figure 2 and their instructions are described in detail in Section 2.3. The sequence of the tasks
169 was the same throughout all blocks.

170 We kept the luminance of the desktop background and the room illumination constant at 52 cd/m²
171 during the whole experiment to prevent that the performances of the eye-trackers were affected by changes
172 in ambient light intensity. Therefore, the calibration procedure and all tasks except the Pupil Dilation
173 task (Section 2.3.9) were presented using a gray background.

174 **2.2 Methods of Data Analysis**

175 For our analysis we built a flexible and modular pipeline that transforms raw eye-tracking data of two
176 eye-trackers to dataframe-based data structures. One dataframe for the data samples, including timestamps,
177 gaze points, velocities, pupil areas and type (saccade, fixation, blink). One dataframe for the eye-tracking
178 events, e.g. fixations, saccades, blinks etc., and one dataframe for the experimental trigger messages which

²The instruction texts can be found on GitHub <https://github.com/behinger/etcomp/tree/master/experiment/Instructions>

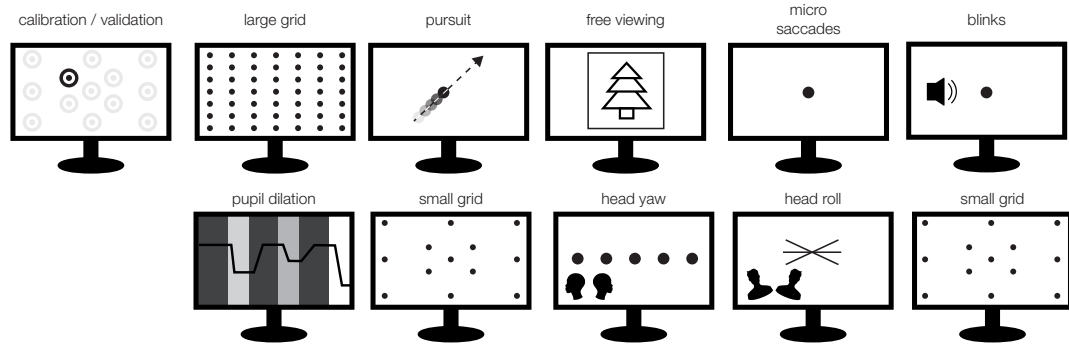


Figure 2. Each block starts with calibration phase and is followed by a fixed sequence of the 10 tasks. The experiment consisted of 6 identical blocks. Thus, each participant took part in 6 calibration procedures and a total of 60 tasks.

179 describe the conditions of the experiment. The pipeline is modularly programmed and components can be
 180 easily exchanged. For example, it is easy to exchange the eye movement classification algorithms for
 181 event detection (blinks, saccades, and fixations). We hope this will improve the comparison of different
 182 algorithms in the future.

183 **2.2.1 Preprocessing**

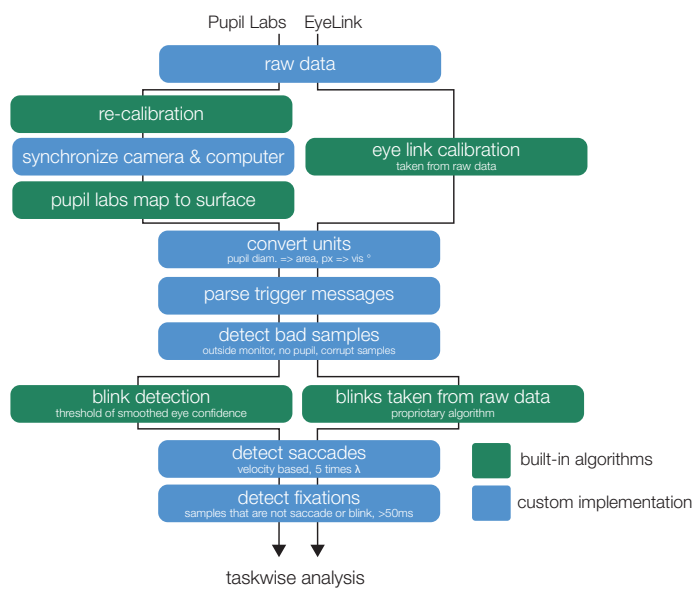


Figure 3. The flowchart illustrates the parallel steps from the recorded raw data to eye movement events (containing information about fixation, saccades, and blinks which are used for the analysis of each task).

184 A flowchart of the eye-tracking preprocessing pipeline is presented in Figure 3. The raw EyeLink
 185 data (maximal manufacturer filter setting) already includes calibrated gaze, mapped to the monitor area
 186 and not much further pre-processing is needed. For Pupil Labs, we were forced to recalibrate the data,
 187 because online during recording, samples from the two eye cameras are not strictly interleaved in time
 188 and can confuse their calibration algorithm. We used the Pupil Labs' Python API (Pupil Labs, 2018, git

189 version: f32ef8e, April 2018) for recalibration and several of the following steps. Due to a (now resolved)
190 bug in Pupil Labs' software, we observed steep linear drifts between eye camera clocks and recording
191 computer clock. Therefore, we recorded at every trigger message, both the current camera timestamp and
192 the recording computer timestamp. Using linear regression, we could then synchronize the eye camera
193 timestamps to the recording computer clock. Note that this step does not eliminate the inherent delay of
194 10 ms of the Pupil Labs' cameras (personal communication with Pupil Labs).

195 Because the Pupil Lab glasses use a world-camera, we next needed to detect the display. For this we
196 displayed 16 screen markers (in principle 4 would be enough, but we could not find a recommendation on
197 how many should be used) in a 2.9° border at the edge of the monitor. These QR-like markers can be
198 detected using the Pupil Labs' API. A rectangular surface is then fitted to these markers and the calibrated
199 gaze is mapped onto the surface using the pupil labs API. Only samples that are mapped to points inside
200 the surface were considered in further analysis.

201 Next, for both eye-trackers, we converted the x (and y) gaze points of the raw samples from screen
202 coordinates in pixels, to spherical angles in degree (with a reference system centered on the subject).

203 $\beta_x = 2 \cdot \text{atan2}(p_x \cdot m, d)$, where β_x denotes the azimuth angle (equivalent to the horizontal position) of
204 the gaze points in visual degrees from the monitor center, p_x denotes the horizontal position relative to the
205 center of the monitor in pixel, m denotes the unit conversion of pixel to mm of the monitor, and d denotes
206 the distance to the monitor in mm. This new spherical coordinate system puts the subject at its origin.
207 The radius of the sphere is the subject to monitor distance. The screen itself would be typically at 90°
208 polar and 0° azimuthal, for convenience of plotting and interpretation, we label the screen's center at 0° ,
209 0° but perform all important calculations in the correct coordinate system (see 2.2.3).

210 We then detected and removed all bad samples that we did not consider in further analysis with the
211 following exclusion criteria: no pupil detected, the gaze point was outside the monitor or the sample was
212 marked as corrupt by the eye-tracker.

213 The experimental triggers that were sent from the stimulus computer to each of the recording computers
214 were parsed into a pandas dataframe. Because recording computer clocks show drift over time relative to
215 each other, we synchronized the timestamps of both eye-trackers by estimating the slope differences at
216 the common event triggers. In addition we corrected a 10 ms constant delay of the Pupil Labs glasses
217 which compensated for their frame-capture delay (personal communication with Pupil Labs, verified
218 using cross-correlation on 2 participants and visual inspection of overlaid signals).

219 **2.2.2 Eye movement classification / detection**

220 It is difficult to establish what an eye movement is, as the definition typically depends on the used
221 algorithm. Because here we focus on the comparison between devices, and an evaluation of algorithms
222 defining fixations is beyond the scope of the present study, we used identical algorithms for both eye-
223 trackers wherever possible. We first detect blinks and subsequently use a velocity based saccade detection
224 algorithm (Engbert and Mergenthaler, 2006) to find saccades. Every sample that is neither a blink or a
225 saccade sample is defined as a fixation sample (see Section 2.2.2). Although, the further comparison of
226 algorithms is outside of the scope of this paper, we want to highlight that our modular analysis pipeline
227 greatly facilitates such comparisons.

228 **Blink detection** For the Pupil Labs data we used the Pupil Labs blink detection algorithm with minor
229 adjustments. Pupil Labs detects blinks based on time-smoothed confidence values of the samples which
230 (in the version used in this paper) reflects the ratio of border pixels of the thresholded pupil overlap
231 with a fitted ellipse. The Pupil Labs blink detection algorithm uses a thresholded smoothed differential
232 filter-output to detect large changes in confidence and thereby identifies the start and the end of blinks.
233 We noticed that the blink detection algorithm sometimes detected very long blinks (tens of seconds)
234 and added a criterion that a blink can only have a start time point if it also has an end time point. Our
235 code-change was that in case we found multiple consecutive blink start point candidates, we only used the
236 last one. For the EyeLink data, we used the blinks that were already detected by its proprietary algorithm
237 during recording.

238 For the subsequent saccade detection, we regarded the samples ± 100 ms around a detected blink
239 event as additional blink samples (Costela et al., 2014) and accounted for them during saccade detection.
240 For the task analyses which rely directly on sample data, we excluded all blink samples.

241 **Engbert and Mergenthaler Saccade Detection** We used the velocity based saccade detection algo-
242 rithm proposed by Engbert and Kliegl (2003); Engbert and Mergenthaler (2006) in the implementation by

243 Knapen (2016). Velocity based saccade detection algorithms use the velocity profile of eye movements
 244 to extract saccade intervals. The algorithm was originally developed to identify microsaccades, but by
 245 adjusting the hyperparameter (λ), it can be used for general saccade detection (for more details see
 246 Engbert and Mergenthaler, 2006).

247 The implementation we used requires a constant sampling rate, and we first interpolated the samples
 248 recorded by the Pupil Labs glasses with piecewise cubic hermite interpolating polynomials to obtain
 249 samples at a sampling rate of 240 Hz. Subsequently, the detected saccade timings were applied to the
 250 individual (non-interpolated) samples. We did not interpolate the EyeLink data samples as the sampling
 251 rate is constant at 500 Hz or constant at 250 Hz. For all saccade detections we used a λ of 5.

252 **Detection of fixations** We labeled all samples as fixation samples that were neither classified as blink
 253 nor saccade samples. We removed all fixation events shorter than 50 ms.

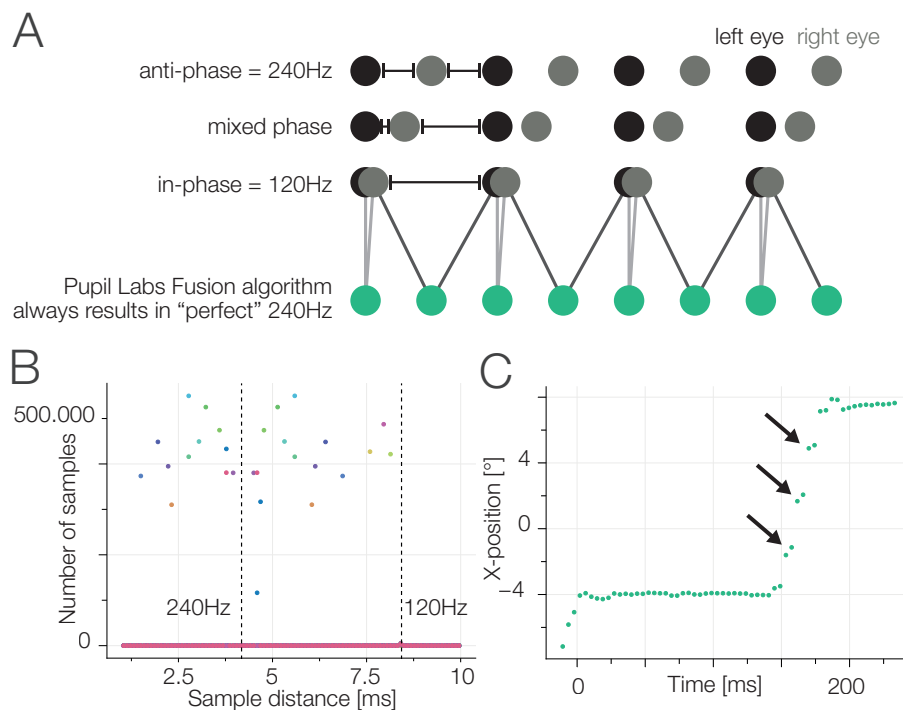


Figure 4. A) Sketch of binocular recording. Two cameras take samples of the eyes. Each has a fixed (and reliable) sampling rate of 120 Hz. During startup, the relative phase of the sampling timepoints of the two cameras is random. If we use the Pupil Labs fusion algorithm (green samples), which pairwise uses the eye-cameras' samples, we will always get a steady sampling rate of 240 Hz regardless of the actual information content. B) Using the eye-camera timestamps we calculate inter-sample time distances (shown also in A). Perfect anti-phasic behavior should show as a cluster around the 240 Hz line, perfect phasic behavior as a cluster around 120 Hz. Mixed phase seems to be the rule. C) The consequence of a bad eye fusion algorithm. Inline with the temporal averaging shown in A) the gaze position is also linearly interpolated. Nevertheless, we often observed staircase like patterns (see also Section 3.4). We think this is due to the 4D binocular calibration function that does not take time-delays into account during the fit.

254 **Notes on sampling frequencies** The EyeLink 1000 was sampled monocularly with 500 Hz for 10
 255 participants and due to a programming mistake with 250 Hz for the other 5 participants. Both Pupil Labs
 256 eye cameras sampled each with 120 Hz. Our eye camera wise inter-sample distances confirm very reliable
 257 rates of 120 Hz. After the fusion and mapping to gaze-coordinates, Pupil Labs reports a sampling rate
 258 of 240 Hz. But this is not the effective sampling rate: The eye cameras are not synchronized to sample

259 in anti-phase to each other (see Figure 4). In our data, we found a uniform phase relation, indicating
260 that participants' effective sampling rates range from close to 120 Hz to close to 240 Hz. In addition,
261 we found two types of artifacts. One is visible in Figure 5, which occurred for some subjects and has
262 an unknown origin. Another (possibly related) artifact has a stereotypical step-function appearance
263 which is especially visible during saccades (see Figure 4). Both artifacts are likely problematic for the
264 velocity-based saccade detection algorithm. For the latter, we offer an explanation of possible origin:
265 During calibration, a 4D to 2D polynomial regression function is fitted. In order to do so, pairs of
266 eye-coordinates (x-y from both cameras, making up the 4D vector) are mapped to the coordinates of a
267 reference point of the world camera. This is done by finding the individual eyes' sample that is closest
268 in time to the target sample. This calibration fit will implicitly compensate for the delay of the two
269 eye signals (except in the case of an in-phase relation). This in itself is suboptimal (as samples of two
270 different time points and thus eye positions are combined), but not alone the cause of the artefact. During
271 gaze production, that is the application of the fitted polynomical function, samples are combined in a
272 alternating fashion (Figure 4A, green dots). The resulting timesample is always the average between
273 the alternating eye samples and thus, as discussed before, has a perfect 240Hz temporal distance. This
274 effectively corrects again for the time-difference between eye camera samples, thereby introducing the
275 step-like artifact. Disclaimer: We tried to be thorough in our investigation, but we are still unsure of the
276 source of the artifact. It is certainly possible that other factors play a role and further simulations should
277 be undertaken to pin down the exact source. We think eliminating this artifact could noticeably improve
278 the performance of the Pupil Labs eye-tracker in the binocular recording condition, but this is outside the
279 scope of the present paper.

280 **2.2.3 Measures of gaze data quality**

281 **Spatial Accuracy in visual angle** The spatial accuracy of an eye-tracker refers to the distance of the
282 measured gaze point and the actual target point (Holmqvist et al., 2012). We calculated this angular
283 difference by the cosine distance between two vectors: the mean gaze point ($f = \begin{pmatrix} f_x \\ f_y \end{pmatrix}$) and target location
284 ($t = \begin{pmatrix} t_x \\ t_y \end{pmatrix}$). For this calculation, we converted the vectors from the Spherical coordinate system to the
285 Cartesian one, which allows us to use the formula for the cosine distance: $\theta = \arccos\left(\frac{f \cdot t}{\|f\| \|t\|}\right)$. After
286 conversion from radians to degrees, this results in the angular difference between 0° and 180°. For the
287 conversion from spherical coordinates to cartesian, we rotated the polar and azimuthal angle by 90°
288 so that the center of the screen is not at <0°, 0°, 60cm> but at <90°, 90°, 60cm> and consequently
289 differences in both polar and azimuthal angle influence the angular distance equivalently.

290 During the calibration procedure the distance between subsequent dots might be larger. Participants
291 typically make catch-up saccades for saccades with large amplitude and small eye movements during
292 fixation periods. Therefore, the gaze data might contain several candidate fixations for analysis. Holmqvist
293 (2017) showed that the selection procedure is uncritical and we decided to use the last ongoing fixation,
294 right before the participants confirmed fixation by pressing the space bar.

295 Our reported aggregate measure of accuracy is the 20% winsorized mean (Wilcox, 2012) spherical
296 angle between the displayed target and the estimated participant's fixation location.

297 **Spatial Precision** Spatial precision refers to the consistency of samples. A good precision is reflected
298 by a small dispersion of samples, as the distances between the samples are small when the samples are
299 close to each other. We make use of the two most popular spatial precision measures, root mean squared
300 (RMS) and the standard deviation.

301 The proximity of consecutive samples is assessed with the root mean square (RMS) of inter-sample
302 distances: Let $d\left(\begin{pmatrix} x_i \\ y_i \end{pmatrix}, \begin{pmatrix} x_{i-1} \\ y_{i-1} \end{pmatrix}\right)$ denote the angular distance (see Section 2.2.3) between sample $\begin{pmatrix} x_i \\ y_i \end{pmatrix}$ and
303 $\begin{pmatrix} x_{i-1} \\ y_{i-1} \end{pmatrix}$. Precision was calculated as:

$$\theta_{RMS} = \sqrt{\frac{1}{n} \sum_{i=1}^n d\left(\begin{pmatrix} x_i \\ y_i \end{pmatrix}, \begin{pmatrix} x_{i-1} \\ y_{i-1} \end{pmatrix}\right)^2}$$

304 The spatial spread is assessed with the standard deviation of the sample locations. The standard
305 deviation for a set of n data samples is calculated as: Let $d\left(\begin{pmatrix} x_i \\ y_i \end{pmatrix}, \begin{pmatrix} \bar{x} \\ \bar{y} \end{pmatrix}\right)$ denote the angular distances between
306 the mean fixation location $\begin{pmatrix} \bar{x} \\ \bar{y} \end{pmatrix}$ (with $\bar{x} = \frac{1}{n} \sum x_i$) and each fixation sample.

$$\theta_{sd} = \sqrt{\frac{1}{n} \sum_{i=1}^n d\left(\left(\begin{matrix} x_i \\ y_i \end{matrix}\right), \left(\begin{matrix} \bar{x} \\ \bar{y} \end{matrix}\right)\right)^2}$$

304 We report fixation spread measured by 20% winsorized average values of standard deviation or
305 inter-sample-distance measured by root-mean-square (RMS).

306 **Pupil dilation** In Task 2.3.9, we measure the pupil size of the participants as a reaction to different
307 luminance stimuli. Measuring the pupil size can be done by means of diameter (Pupil Labs glasses) or
308 pupil area (EyeLink 1000). With the Pupil Labs glasses, pupil diameter is estimated from a fitted ellipse.
309 With the EyeLink 1000, pupil area is calculated as the sum of the number of pixels inside the detected pupil
310 contour. We converted the pupil diameters reported by Pupil Labs into pupil area using: $A = \frac{1}{4}\pi \cdot l_1 \cdot l_2$
311 where A denotes the ellipsis area, l_1 denotes the semi-major axis and l_2 denotes the semi-minor axis. In
312 our experiment, pupil area is reported in pixels or arbitrary unit. The absolute pupil size is not important
313 for the current study and due to lacking pupil calibration data, a conversion to mm is not possible. Pupil
314 size fluctuates globally over blocks due to attention or alertness. We normalized the pupil area to the
315 median of a baseline period (see Section 2.3.9).

316 **2.3 Tasks**

317 **2.3.1 Task sequence**

318 The task sequence was kept the same in all blocks and across all participants (see Figure 2). At the
319 beginning of each block, directly after the eye-tracker calibration, we presented a grid task, that was
320 designed to assess the spatial accuracy of the eye-trackers. In addition we used the grid task right
321 before and after a controlled block of head movements. Furthermore, we placed the fixation heavy tasks
322 (Microsaccade task 2.3.7 and Pupil Dilation task 2.3.9) in between tasks which were more relaxing for
323 the participants (Blink task 2.3.8, Free viewing task 2.3.6, Accuracy task 2.3.4).

324 **2.3.2 Fixation Targets**

325 Throughout the experiment, we used three different fixation targets: For manufacturer calibration/validation,
326 we used concentric circles following the Pupil Labs specifications in order to detect reference points from
327 the world camera. For most fixation tasks we used a fixation cross that was shown to reduce miniature eye
328 movements (Thaler et al., 2013). For several tasks, we used a bullseye (outer circle: black, diameter 0.5°,
329 inner circle: white, diameter 0.25°): Firstly, for smooth pursuit because diagonal fixation dot movement
330 looked better aesthetically. Secondly, for microsaccades, as we did not want to minimize microsaccades.
331 Thirdly, for pupil dilation we could keep the bullseye visible regardless of background illumination.

332 **2.3.3 Calibration**

333 Since the experiment was designed to evaluate the performance of the eye-trackers, we calibrated
334 the devices at the beginning of each block. Calibration was performed using a 13 point randomized
335 calibration procedure. We used concentric rings as fixation points which can be detected by the Pupil
336 Labs glasses' world camera. The 13 calibration points were selected as a subset of the large grid from the
337 accuracy task (see Section 2.3.4). Fixations were manually accepted by the experimenter. An automatic
338 procedure (EyeLink default setting) was not possible, because the calibration of both recording devices
339 was performed at the same time. After calibration, a 13 point verification was performed which was
340 identical in procedure but with a new sequence. The accuracies were calculated online by both devices.
341 The devices were recalibrated if necessary, until the mean validation accuracies met the recommendations
342 by the manufacturers. The mean validation accuracy limit for the EyeLink 1000 was 0.5° where the
343 validation accuracy of each point was not allowed to exceed 1° (SR-Research manual). The mean
344 validation accuracy limit for the Pupil Labs glasses was 1.5° (personal communications with Pupil Labs).
345 If more than 10 unsuccessful calibration attempts were made, with adjustments of the eye-trackers in
346 between, we stopped the recording session and excluded the participant from the experiment.

347 **2.3.4 Task 1 / Task 7 / Task 10: Accuracy task with the large and the small grid**

348 We used a fixation grid to evaluate the difference between the location of a displayed target and the
349 estimated gaze point. We estimated absolute spatial accuracy and in addition, decay of the calibration
350 accuracy over time. We used two variants of the accuracy task, a large grid based on a 7×7 grid and a
351 small grid based on a subset of 13 points. The large grid accuracy task is shown directly after the initial

352 calibration of each block. This allowed us to estimate the accuracy of the eye-trackers with almost no
353 temporal decay. To additionally investigate the decay of the calibration, we recorded the small grid tasks
354 after the participant completed 5 different tasks (after about 2/3 of the block $\approx 4\text{ min } 42\text{ s}$) and after 2
355 further tasks involving head movements ($\approx 6\text{ min } 18\text{ s}$).

356 **Task with the large grid:** The participants were instructed to fixate targets that appeared at one of
357 the 49 crossing points of a 7×7 grid. The crossing points were equally spaced in a range from -7.7° to
358 7.7° vertically and -18.2° to 18.2° horizontally. At each crossing point a target appeared once, so in total
359 49 targets were shown during every task repetition. The participants were asked to saccade to the target
360 and fixate it, and once they felt their eyes stopped moving, to press the space bar to continue. The center
361 point was used as the start and end point.

362 A sample screen is visible in Figure 1 and an animated gif is available on GitHub (<https://github.com/behinger/etcomp/tree/master/resources>).

364 **Task with the small grid:** The small grid task is analogous to the large grid task, but with a subset of
365 13 target points. These points were also used in the calibration procedure and spanned the whole screen.

366 **Randomization of the large grid:** A naive approach of randomization of the sequence of fixation
367 points would lead to heavily skewed distributions of saccade amplitudes. Therefore, we used a constrained
368 randomization procedure to expose participants to as-uniform-as-possible saccade amplitudes and angles
369 distributions. We used a brute-force approach maximizing the entropy of the saccade amplitude histogram
370 (17×1 degree bins) and the saccade angle histogram (10×36 degree bins) with an effective weighting
371 (due to different bin widths) of 55% to 45%. This allowed for better subject comparisons as the between-
372 subject-variance due to different saccade parameters is minimized with this procedure.

373 **Randomization of the small grid:** The sequence of the target positions was naively randomized
374 within each block and for each participant.

375 **Measures of the large grid:** For the large grid we evaluated how accurate the participants fixated
376 each target, that is the offset between the displayed target and the mean gaze position of the last fixation
377 before the new target is shown (see Section 2.2.3). Furthermore, we analyzed the precision of the fixation
378 events by evaluating the RMS and SD (see Section 2.2.3).

379 **Measures over all grid tasks:** Because we recorded grid tasks at several time points during a
380 block, we were able to obtain accuracy measures with no decay (directly after initial calibration), af-
381 ter some temporal drift (2/3 of the block elapsed), and after provoked head movements (yaw and roll
382 task 2.3.10). The accuracy decay over time showed effects for which statistical significance could
383 not directly be seen. Therefore, after plotting the data, we decided to use a robust linear mixed ef-
384 fects model with conservative Walds t-test p-value calculation ($\text{df} = \text{Nsubjects}-1$). We used the robust
385 version as we found out (after inspecting the data) that there are outliers at all levels, single element,
386 blocks and subjects. These are accommodated by the winsorized means in the general analysis, but
387 not if we would have performed a normal linear mixed model (LMM). For this we defined the LMM
388 accuracy $\sim (1 + \text{et} * \text{session} + 1 | \text{subject} \backslash \text{block})$ and evaluated it with the robustlmm R
389 package (Koller, 2016). The maximal LMM containing all random slopes did not converge and therefore
390 we used the simplified model as stated above.

391 **2.3.5 Task 2: Smooth Pursuit**

392 Smooth pursuit is a common eye movement that occurs when the oculomotor system tracks a moving
393 object. It is especially common while we move relative to a fixated object and, therefore, elemental to
394 detect reliably for mobile settings. Because automatic smooth pursuit detection is still in its infancy, we
395 opted to use a parametric smooth pursuit task that can be evaluated with a formal model.

396 **Task:** To analyze smooth pursuit movements, we followed Liston and Stone (2014) and adapted
397 their variant of the step-ramp smooth pursuit paradigm. The participants fixated a central target and
398 were instructed to press the space bar to start a trial. In this task we used a bullseye fixation target. The
399 probe started after a random delay. The delay was sampled from an exponential function with a mean of
400 0.5 s with a constant offset of 0.2 s and truncated at 5 s. This results in a constant hazard function and
401 counteracts expectations of motion onset (Baumeister and Joubert, 1969). The stimuli were moving on
402 linear trajectories at one of 5 different speeds (16, 18, 20, 22, 24 $^\circ/\text{s}$). The trial ended once the target was
403 at a distance of 10 $^\circ$ from the center. We used 24 different orientations for the trajectories spanning 360 $^\circ$.
404 To minimize the chance of catch-up saccades, we chose the starting point for each stimulus such that it
405 took 0.2 s for the target to move from the starting point to the center. We instructed the participants to
406 follow the target with their eyes as long as possible.

407 **Randomization:** One block consisted of 20 trials with a total of 120 trials over the experiment. Each
408 participant was presented with each of the 120 possible combinations of speed and angle once, randomized
409 over the whole experiment.

410 **Measures:** To analyze smooth pursuit onsets and velocities we generalized the model used by Liston
411 and Stone (2014) to a Bayesian model (see also Figure 8B). First, we rotated the x-y gaze coordinates
412 of each trial in the direction of the smooth-pursuit target. Now an increase in the first dimension is an
413 increase along the smooth-pursuit target direction. We then restricted our data fit to samples up to the first
414 saccade exceeding 1° (a catch-up saccade) or up to 600 ms after trial onset. We used the probabilistic
415 programming language STAN to implement a restricted piece-wise linear regression with two pieces. The
416 independent variable of the regression is the eye position along the smooth pursuit trajectory which should
417 be a positive component (else the eye would move in the opposite direction to the smooth pursuit target).
418 The first linear piece is constrained to a slope of 0 and a normal prior for the intercept with mean 0 and SD
419 of 1° (in the rotated coordinate system). The hinge or change-point has a prior of 185 ms post-stimulus
420 onset with a SD of 300 ms. The slope of the second linear piece is constrained to be positive and follows
421 a 0-truncated normal distribution with mean 0 and SD of 20°/s. The noise is assumed to be normal with a
422 prior SD of 5°. For the hinge we used a logistic transfer function to allow for gradient-based methods to
423 fit the data. We want to note that this analysis is sensitive to detecting the initial saccade correctly and
424 does not distinguish between catch-up saccades and initial reaction saccades. For this paper, we assume
425 that the impact of these inadequacies can be compensated by the robust winsorized means that we employ
426 at various aggregation levels. For each trial we take the mean posterior value of the hinge-point and the
427 velocity parameter and use winsorized means over blocks and subjects to arrive at our group-level result.
428 In addition, we count the detected number of saccades during the movement of the target.

429 **2.3.6 Task 3: Free Viewing**

430 **Task:** For the Free Viewing task, we presented photos of natural images consisting mostly of patterns
431 taken from Backhaus (2016), a thesis evaluating SMI mobile eye-tracking glasses against an Eyelink 1000.
432 Participants fixated on a central fixation cross for on average 0.9 s with a uniform random jitter of 0.2 s
433 prior to the image onset. The participants were instructed to freely explore the images. During each of the
434 6 blocks, we showed 3 images (900 × 720 pixels) for 6 s, thus 18 different images in total.

435 **Randomization:** The order of the 18 images was randomized over the experiment and each image
436 was shown once. Due to a programming mistake, the first participant saw 5 different images compared
437 with the other participants. These deviant images were removed from further analysis.

438 **Measures:** We compared the number of fixations, fixation durations, and saccadic amplitudes between
439 eye-trackers. Furthermore, we visually compared the gaze trajectories of the two eye-trackers to get
440 an impression of the real world effects of spatial inaccuracies. We excluded the first fixation on the
441 fixation cross. For the central fixation bias we smoothed a pixel-wise 2D histogram with a Gaussian
442 kernel (SD = 3°).

443 **2.3.7 Task 4: Microsaccades**

444 **Task:** In order to elicit microsaccades, we showed a central fixation target for 20 s. The participants
445 were instructed to continue the fixation until the target disappeared. In this task, we used the bullseye
446 fixation target and for obvious reasons, not the fixation target that minimizes microsaccades.

447 **Measures:** We evaluated the number of microsaccades, the amplitudes of the microsaccades, and the
448 form of the main sequence. For this task, we ran the Engbert algorithm (Engbert and Mergenthaler, 2006)
449 only on this subset of data specifically for each block.

450 **2.3.8 Task 5: Blink task**

451 **Task:** The participants fixated a central fixation target and were instructed to blink each time they
452 heard a beep. The 300 Hz beep sound chimed 100 ms for 7 times with a pause of 1.5 s between every beep.
453 Each sound onset was uniformly jittered by ±0.2 s. We used the Psychophysics Toolbox's MakeBeep
454 function to generate the sound.

455 **Measures:** We evaluated the number of detected blinks and blink durations. Note that different blink
456 detection algorithms were used (see Section 2.2.2).

457 **2.3.9 Task 6: Pupil Dilation task**

458 **Task:** In this task, we varied the light intensity of the monitor to stimulate a change of pupil size.
459 During the entire task, a central fixation target was displayed which the participants were instructed

460 to fixate. Each block consisted of 4 different monitor luminances (12.6, 47.8, 113.7 and 226.0 cd/m²)
461 corresponding to 25%, 50%, 75% and 100%. Before each target luminance, we first showed 7 s (jittered
462 by ± 0.25 s) of black luminance (0.5 cd/m², 0%). This was done in order to allow the pupil to converge to
463 its largest size. Then, one of the 4 target luminances was displayed for 3 s (jittered by ± 0.25 s).

464 **Randomization:** The order of the four bright stimuli was randomized within each block.

465 **Measures:** We analyzed the relative pupil areas per luminance. We first converted the Pupil Labs
466 pupil signal from diameter to area (see Section 2.2.3). Then we calculated the normalized pupil response
467 by dividing through the median baseline pupil size 1 s prior to the bright stimulus onset. We did this as
468 visual inspection of raw traces showed that in many trials the 7s black luminance was not sufficient to get
469 back to a constant baseline and in other trials the pupil seemed converged, but not on the same baseline
470 level indicating either block-wise attentional processes, different distance of eye camera to eyes or other
471 influences. The normalized pupil area is therefore reported in percent area change to median baseline.

472 **2.3.10 Task 8/9: Head Movements**

473 **Task roll movement:** In this task, we examined the gaze data while the participants tilted their heads.
474 The participants saw a single rotated line in each trial. In each trial the line was presented at 8 different
475 orientations (-15° , -10° , -5° , 0° (horizontal), 5° , 10° , 15°). The participants were instructed to rotate
476 their head so that their eyes are in line with the line on the screen, while fixating the target. Once the
477 participants aligned their eyes with the line, they pressed the space bar to confirm the fixation/position
478 and the next line was shown.

479 **Randomization for roll movement:** The sequence of the lines was randomized within each block
480 and for all participants. The order of the roll and yaw tasks alternated in each block for a participant. Half
481 of the participants started with the roll task, the other half with the yaw task.

482 **Measures for roll movement:** Because the subjects continued to fixate on the fixation cross at the
483 center of the line and rolled their head, often no new fixation was detected. Therefore, we analyzed the
484 winsorized average fixation position 0.5 s before the button press.

485 **Task yaw movement:** In this task the participant performed 15 yaw movements during one block.
486 For this purpose we showed targets at 5 equally spaced positions on a horizontal line (Positions: -32.8° ,
487 -16.7° , 0° , 16.7° , 32.8°). The participants were instructed to rotate their head so that their nose points to
488 the target and then fixate it. Once they fixated the target, they pressed the space bar to confirm the fixation
489 and the next target appeared.

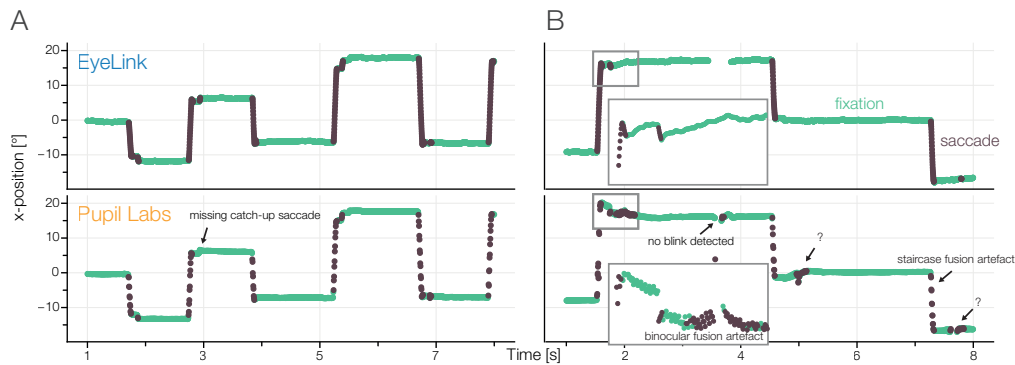
490 **Randomization for yaw movement:** The positions of the 15 targets were randomized within one
491 block.

492 **Measures for yaw movement:** We analyzed the accuracy of the estimated gaze point of the participant
493 on the last fixation before subjects confirmed the yaw movement.

494 3 RESULTS

495 We recorded the eye gaze position and pupil diameter of 15 participants concurrently with two eye-trackers.
496 In Figure 5, we show exemplary traces of a single participant for both eye-trackers. We see an overall
497 high congruence of the recorded samples. Often even small corrective saccades seem to match between
498 the two eye-trackers. But of course, important information which cannot be observed visually is hidden in
499 the traces and requires quantitative analyses.

500 Note that for the results in the following, we generally first calculated the winsorized mean for each
501 participant over blocks and then report a second winsorized mean and the inter-quartile range (IQR) over
502 the already averaged values. In other words, we report the IQR of means, not the mean IQR.



503 **Figure 5.** Annotated samples from the accuracy task (fixations: green, saccades: dark)
504 for A) a good subject and B) a subject with pupil labs artifacts

505 3.1 Results: Calibration

506 In the great majority of eye-tracking experiments, eye-trackers first have to be calibrated. That is,
507 (typically) a mapping from a pupil position coordinate frame to a world coordinate frame needs to be
508 estimated. We used an experimenter-paced 13 point calibration procedure to calibrate both eye-trackers
509 simultaneously. We made use of the eye-trackers' internal validation methods.

510 For EyeLink, the winsorized mean validation accuracy was 0.35° (IQR: 0.31° to 0.38°), for Pupil Labs
511 it was 1.04° (IQR: 0.96° to 1.14°). These results are certainly biased as a selection bias was introduced
512 when we repeated the calibration if the validation accuracy was worse than our prespecified validation
513 accuracy limits (0.5° for EyeLink 1000 and 1.5° for Pupil Labs glasses). Besides the subjects that were
514 completely excluded from further analysis (see 2.1.1), only for 7 validations (of in total $6 \cdot 15 \cdot 2 = 180$
515 eye-tracker validations) a validation below the limits was not possible (see Figure 6 C, D). Note that these
516 7 validations are equally spread over eye-trackers and are uncorrelated over eye-trackers/sessions. For
517 unknown reasons, the Pupil Labs validation data was not saved for 3 participants.

518 In summary, we succeeded in calibrating both eye-trackers simultaneously in the validation accuracy
519 ranges that are recommended by the eye-tracker manufacturers.

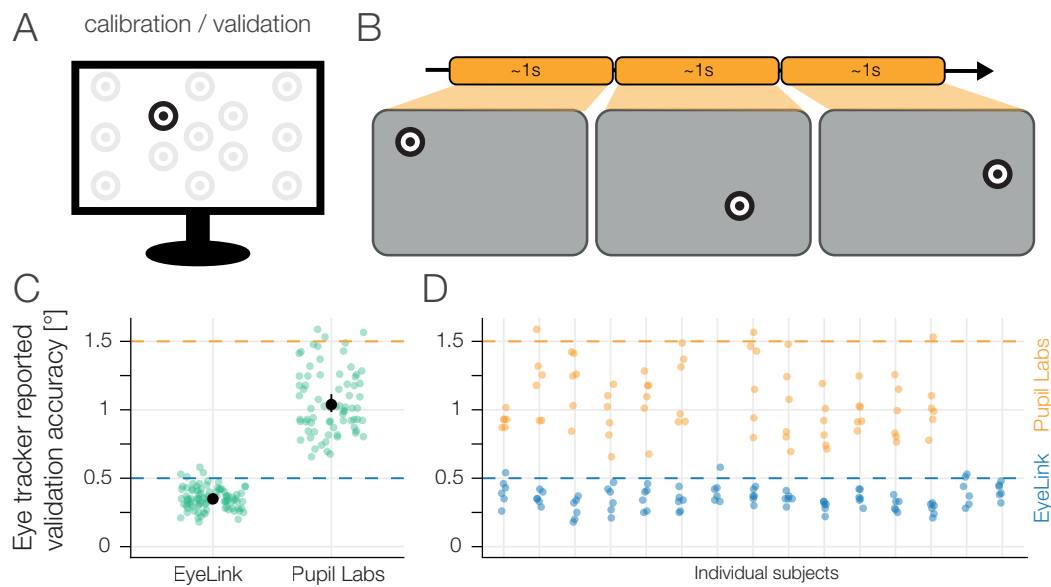


Figure 6. A) Calibration Validation display. B) A 13 point calibration procedure paced by the experimenter was performed at the beginning of each block. During calibration the built-in procedure of each eye-tracker was used. Both eye-trackers were calibrated simultaneously. C) Reported 13 point validation accuracy of the eye-trackers' built-in procedures with winsorized mean and 95% winsorized mean confidence intervals. Note that we show disaggregate data over participants and report mean and CI over blocks instead. The values aggregated over participants first are reported in the text. D) Reported 13 point validation accuracy of the eye-trackers' built-in procedures split over participants (same data as in C). Each point indicates the accuracy value for one participant in one block. Calibration accuracy data of Pupil Labs was missing for 3 participants. The prespecified accuracy limits (see Section 2.1.3) were exceeded in only 7 out of 180 validations without resulting in a recalibration.

518 3.2 Results Task 1 / 7 / 10: Accuracy task with small grid I and II

519 Spatial accuracy and precision are the most common benchmark parameters of eye-trackers. We measured
 520 those by asking subjects to fixate points on a 49 point fixation grid. In order to record the best-case spatial
 521 accuracy and precision we employed this task immediately after calibration. We report 20%-winsorized
 522 means, first aggregated over the 49 grid points, then over the 6 blocks and finally over the 15 participants.

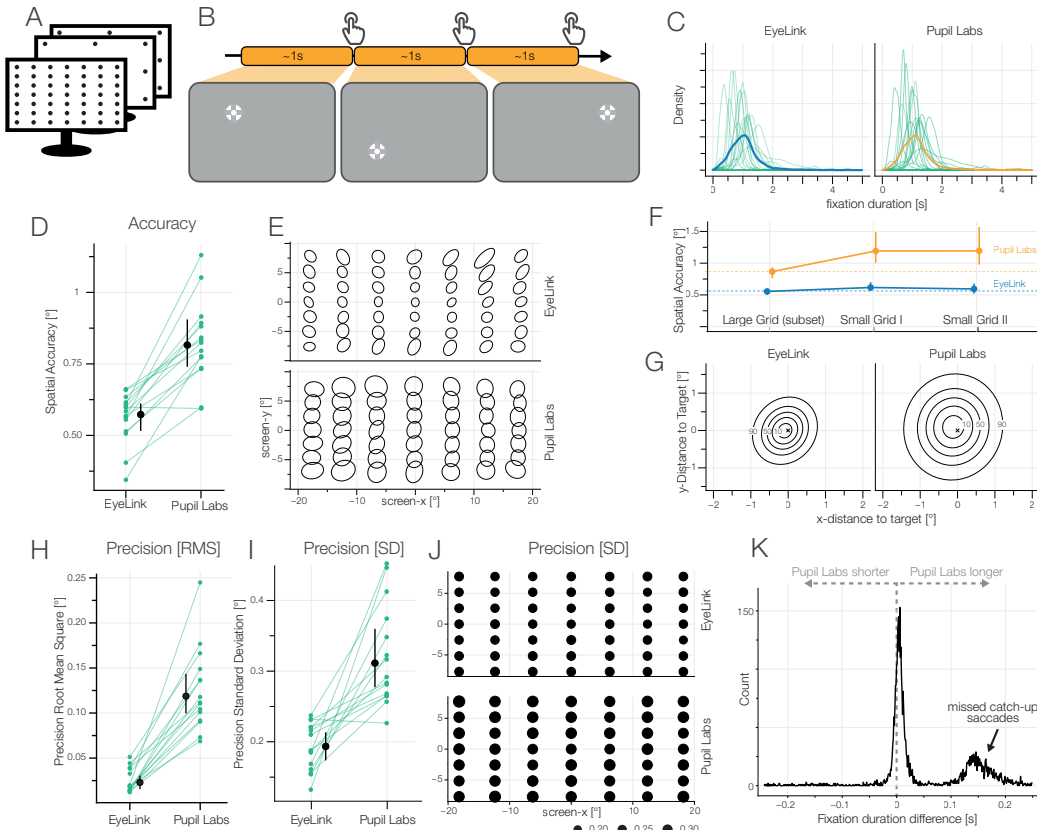


Figure 7. A) Accuracy task. B) The participants fixated single points from a 7×7 grid and continued to the next target self-paced by pressing the space bar. The last fixation during pressing the space bar was used for analysis. C) Kernel densities of fixation durations. The thick line indicates the average over all data points irrespective of subjects. D) Spatial accuracy: 20% winsorized mean and between subject 95% winsorized confidence intervals are shown. Blue lines show 20% winsorized means over 6 blocks, where each block was calculated by the 20% winsorized mean accuracy over 49 grid points. E) 2D-Distribution of fixations around the respective grid points. 95% bivariate t-distribution contours ($df=5$) are shown. That is, a robust estimate where 95% of a grid points' fixations are expected to fall. F) Spatial accuracy over the time of one block. Dashed line shows average at the first measurement point facilitating comparison to the two measurement points. G) Difference of actual fixation position and fixation target position. Bivariate t-distribution contours ($df=5$) over all fixations over all participants. H) Precision: Root mean square (RMS) inter-sample distance. I) Precision: Fixation spread (SD). J) SD over grid point positions. K) Pupil Labs – EyeLink fixation duration difference.

523 The winsorized mean accuracy of EyeLink was 0.57° (IQR: 0.53° to 0.61°), of Pupil Labs 0.82°
 524 (IQR: 0.75° to 0.89°), with a paired difference of -0.25° (CI_{95} : -0.2° to -0.33°). Therefore, Pupil Labs
 525 has in this condition a $\approx 45\%$ worse spatial accuracy value than EyeLink. These accuracies have to be
 526 taken as best-case accuracies as they were measured shortly after the calibration procedure.

527 We quantified the spatial precision using the inter-sample distances (root mean squared) and the

528 fixation spread (standard deviation). For EyeLink the winsorized mean RMS was 0.023° (IQR: 0.014° to 0.04°), for Pupil Labs 0.119° (IQR: 0.096° to 0.143°), with a paired difference of -0.094° (CI_{95} : -0.077° to -0.116°). Therefore, Pupil Labs has a $\approx 500\%$ worse RMS precision than EyeLink. We expect the binocular fusion issues and the differing sampling rates (4) to inflate this measures. The interaction between RMS and sampling rate is complex, as in principle both, increased RMS due to higher sampling rate (because more noise is included; compare Holmqvist et al., 2011) and reduced RMS due to higher sampling rate (because of quadratic summation) are possible.

535 The arguably more intuitive spatial precision measure is standard deviation as it gives an intuitive
536 measure of fixation spread. For EyeLink, the winsorized mean standard deviation was 0.193° (IQR:
537 0.164° to 0.22°), for Pupil Labs 0.311° (IQR: 0.266° to 0.361°), with a paired difference of -0.118°
538 (CI_{95} : -0.073° to -0.174°). Here, similar to accuracy, Pupil Labs shows a $\approx 50\%$ worse precision than
539 EyeLink.

540 We measured a subset of grid points at three points during a block: Immediately after calibration,
541 after 279 s (95-percentile: 206 s - 401 s) and after 375 s (95-percentile: 258 s - 551 s). Because differences
542 are not as evident as in other conditions, a robust linear mixed model was used to estimate the decay in
543 accuracy over time. EyeLink showed a quite stable calibration accuracy. At the second measurement,
544 average accuracy was worse than initial measurement by 0.06° ($t(14)=3.86$, $p=0.002$), at the third
545 measurement, only marginally worse than initial measurement by 0.03° ($t(14)=2.1$, $p=0.05$). In contrast,
546 Pupil Labs showed a much stronger decay. At the second measurement the accuracy dropped already by
547 0.25° ($t(14)=11.27$, $p<0.001$) to $\approx 1.1^\circ$. Interestingly, even after head motions, the accuracy did not get
548 much worse with a difference to the initial measurement of 0.29° ($t(14)=13.07$, $p<0.001$).

549 For EyeLink, we estimated an winsorized average fixation duration on one grid point of 1.03 s (IQR:
550 0.82 s to 1.28 s), for Pupil Labs 1.09 s (IQR: 0.89 s to 1.34 s), with a paired difference of -0.07 s (CI_{95} :
551 -0.06 s to -0.08 s). As clearly evident in Figure 7K, there are two sources for the observed difference.
552 For one, Pupil Labs often misses catch-up saccades, thereby prolonging average fixation duration. On
553 the other hand the initial peak around 0 is positively biased, indicating that also for other fixations, Pupil
554 Labs offers longer fixation durations. This might be a consequence of our use of the sample-wise saccade
555 detection algorithm.

556 In conclusion, we found that EyeLink, as well as Pupil Labs, showed rather good spatial accuracies
557 and precision values. As expected from a gold standard, EyeLink exhibited better performance. A decay
558 of calibration was found only for Pupil Labs, where the calibration decayed by $\approx 30\%$ after 4 min 30 s. It
559 is therefore important to recalibrate the Pupil Labs Glases more often to keep the same level of accuracy
560 and spatial precision as initially after calibration.

561 3.3 Results Task 2: Smooth Pursuit

562 Smooth pursuit is a common eye movement in mobile settings, movies or other dynamic stimuli. It is
563 distinct in its eye motion and physiological origin. To elicit and measure smooth pursuit, we implemented
564 a smooth pursuit test battery proposed by Liston and Stone (2014), with a target moving from the center of
565 the screen outwards using 24 different angles and 5 different speeds. We developed and fitted a single-trial
566 Bayesian model to estimate the tracking onset and the tracking velocity (see Section 2.3.5).

567 For EyeLink the winsorized mean smooth pursuit onset latency was 0.241 s (IQR: 0.232 s to 0.250 s),
568 for Pupil Labs 0.245 s (IQR: 0.232 s to 0.252 s). The estimated onset latencies were equal between
569 eye-trackers with an average difference of -0.001 s (CI_{95} : 0.003 s to -0.007 s). Our analysis method
570 estimates the onset latency using many samples before and after the onset. This could hide potential
571 latency effects without such a structural analysis method.

572 For EyeLink the winsorized mean tracking velocity was $10.5^\circ/\text{s}$ (IQR: $8.5^\circ/\text{s}$ to $12.52^\circ/\text{s}$), for Pupil
573 Labs $13.1^\circ/\text{s}$ (IQR: $11.7^\circ/\text{s}$ to $14.8^\circ/\text{s}$), with a paired difference of $-2.4^\circ/\text{s}$ (CI_{95} : $-1.5^\circ/\text{s}$ to $-4.0^\circ/\text{s}$).
574 These pursuit velocities are much smaller than the target velocities (but accurately estimated, for example
575 see Figure 8D). These slow pursuit velocities are accompanied by a high frequency of catch-up saccades.
576 Specifically, the distance the target is tracked is covered evenly by pursuit movements and catch-up
577 saccades. In addition to the large number of catchup saccades, we observed that Pupil Labs reported
578 smaller catch-up saccade amplitudes, independently of the target velocity (Figure 8 G). If we take the
579 lower sampling rate of the Pupil Labs eye-tracker into account, we see that each catch-up saccade consists
580 of fewer samples (compared to the EyeLink). If we have fewer samples, detected saccades will also exhibit
581 smaller amplitudes (similar to Figure 9F). Consequently, tracking velocities are also biased, as samples

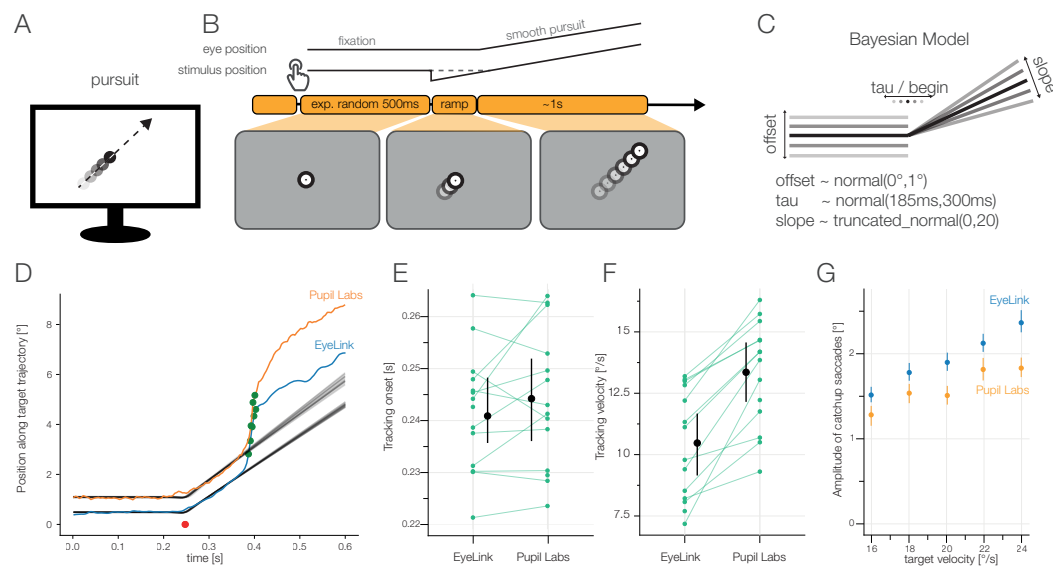


Figure 8. A) Smooth Pursuit task. B) The participants made smooth pursuit eye movements imposed by a step ramp paradigm (see Section 2.3.5). C) Analysis model: Single-Trial Bayesian estimates of a hinge-regression model. The main parameters were the offset of the initial fixation, the tracking onset of the smooth pursuit eye movement and the tracked velocity (slope). Prior to model fit we rotated the data to align all tracking target directions. D) Example model fit: One trial of one participant. We used the data up to a first possible catch-up saccade (green dots). Uncertainty in model fit is visualized by plotting 100 random draws from the posterior. Red dots (overlapping for both eye-trackers) indicate estimated smooth pursuit onset. E) Winsorized average tracking onset for each participant. F) Winsorized average tracking velocities for each participant. G) Amplitudes of catchup saccades. Pupil Labs reports smaller catchup saccade amplitudes independently of target velocity.

582 later in time (and thus with higher eccentricity) are included in the model for Pupil Labs compared to
583 EyeLink. This could explain the bias of the model to fit steeper slopes in Pupil Labs compared to EyeLink.

584 In summary, smooth pursuit signals could be detected by both eye-trackers. There were large biases
585 between eye-trackers, even though the artificial task structure should make smooth pursuit detection easy.

586 3.4 Results Task 3: Free Viewing

587 If subjects inspect images without a specific task, it is usually referred to as free-viewing or unrestricted
588 viewing. Free viewing can be used to find attentional biases, fit saliency models or measure task-unbiased
589 fixation behaviour. We presented a total of 18 images in the Free-Viewing task. The images were displayed
590 for 6 s each and showed mostly natural patterns and textures, and scenarios.

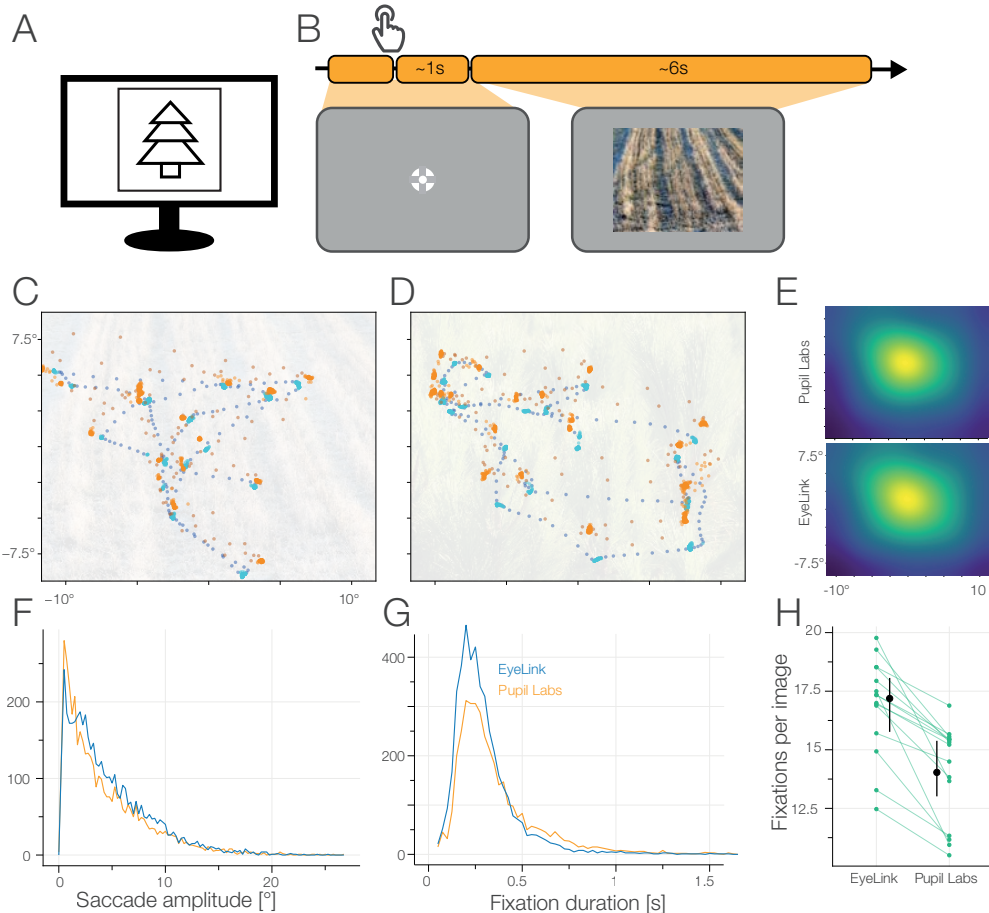


Figure 9. A) Free Viewing task. B) The participants freely explored the images for 6 s. C/D) Scanpaths from one participant (EyeLink: blue; Pupil Labs: orange; fixation samples: brighter color; saccade samples: darker color). E) Heatmaps for EyeLink and Pupil Labs on the base of detected fixations with a Gaussian kernel with 3° smoothing. F) Histogram of saccade amplitude. Binwidth of 0.25° . G) Histogram of fixation duration. Binwidth of 25 ms. H) Winsorized mean number of fixations per image.

591 For EyeLink, the winsorized mean fixation count was 17.2 (IQR: 16.2 to 18.3), for Pupil Labs 14.1
592 (IQR: 12.7 to 15.6). Thus Pupil Labs reported on average 2.5 (CI₉₅: 3.8 to 1.7) fewer fixations per 6 s.
593 For EyeLink, the winsorized mean fixation duration was 0.271 s (IQR: 0.246 s to 0.30 s), for Pupil Labs
594 0.330 s (IQR: 0.310 s to 0.352 s), with a paired difference of -0.054 s (CI₉₅: -0.039 s to -0.072 s). For
595 EyeLink, the winsorized mean amplitude winsorized mean was 4.24° (IQR: 3.63° to 4.89°), for Pupil
596 Labs 3.69° (IQR: 3.15° to 4.28°), with a paired difference of 0.39° (CI₉₅: 0.69° to 0.09°).

597 As shown in Figure 9E, we find the classical central fixation bias (compare Tatler, 2007). In Figure 598 9C,D we show the scan-paths of one participant during the Free Viewing task. The recorded scan-paths 599 from EyeLink and Pupil Labs differ noticeably. Locally, Pupil Labs shows a lower sampling frequency 600 and alternating gaze position (indicating poor fusion of the two eyes' data) resulting in high variance of 601 eye position, especially visible during saccades. Globally, if we would try to align the samples, we see 602 that we would need not only linear transformations, but also and non-linear warps. This hints that already 603 the built-in 2D polynomial calibration routines of both eye-trackers differ in their estimated calibration 604 coefficients, even though they are quite similar from an algorithmic point of view.

605 In contrast to the good performance of both eye-trackers in the accuracy task (Section 3.2), we see 606 significant shortcomings in the Free Viewing analysis. Especially the bad fusion of the eye positions and 607 the high variability of the samples recorded with the Pupil Labs glasses are obvious. In addition, Pupil 608 Labs finds fewer and shorter saccades than EyeLink and therefore on average longer fixation durations. 609 Hence, the eye-tracker should be carefully chosen, if individual eye traces are of importance.

610 3.5 Results Task 4: Microsaccades

611 The eye never stays still but is constantly moving. If saccade-like behavior is found while the subjects 612 subjectively fixates, they are usually termed microsaccades. In order to investigate how well microsaccades 613 can be found, we showed a central bullseye fixation point for 20 s to elicit these microsaccades and 614 analyzed their amplitudes and rates.

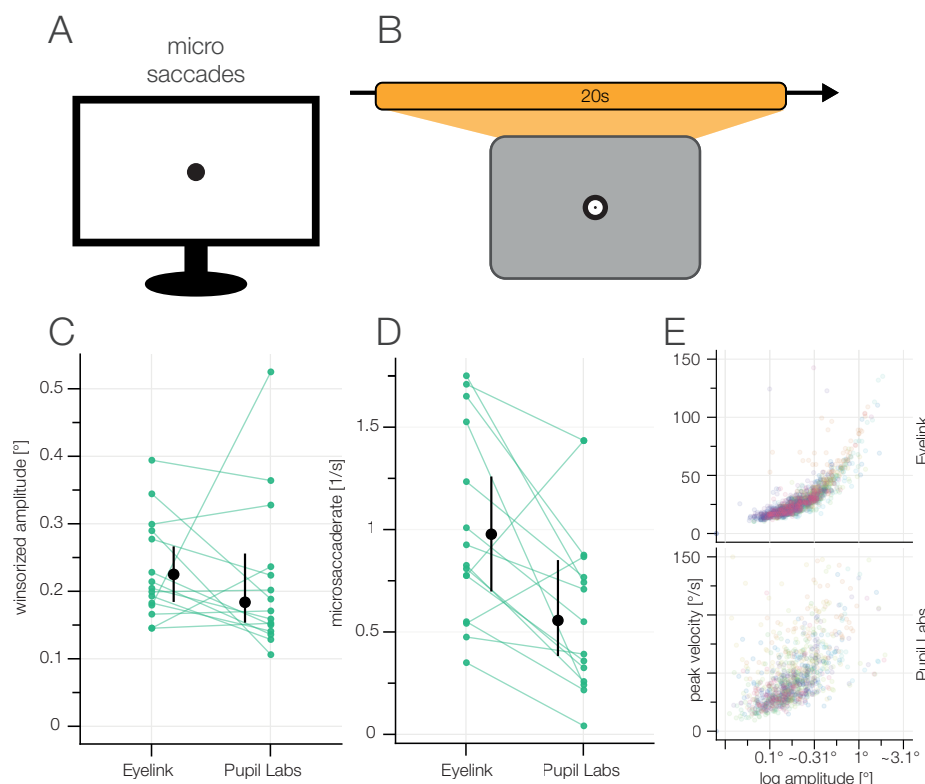


Figure 10. A) Microsaccades task. B) The participants kept fixating a central fixation point for 20 s. C) Microsaccade amplitudes. D) Microsaccade rate. E) Main sequences for both eyetrackers. Different colors depict different subjects.

615 For EyeLink, the winsorized mean amplitude was 0.23° (IQR: 0.18° to 0.28°), for Pupil Labs 0.18° 616 (IQR: 0.15° to 0.23°), with a paired difference of 0.03° (CI_{95} : 0.08° to -0.02°). These microsaccade

617 amplitudes follow what is expected from pupil-estimated microsaccades (Nyström et al., 2016). The
618 microsaccade rate is also in line with previous research (e.g. Winterson and Collewun, 1976; Rolfs, 2009).
619 For EyeLink, the winsorized mean number of microsaccades was 117.2 (IQR: 79.5 to 165.5), for Pupil
620 Labs 66.73 (IQR: 35.0 to 98.0), with a paired difference of 47.0 (CI_{95} : 75.67 to 16.20). This indicates
621 that Pupil Lab finds only $\approx 50\%$ of microsaccades.

622 The main sequence of the Pupil Labs glasses shows much higher variance (Figure 10 E), while the
623 main sequence is cleanly visible in the EyeLink plot. Unsurprisingly, Pupil Labs has problems identifying
624 microsaccades. Even though the amplitudes of detected microsaccades look comparable, the number of
625 microsaccades is much reduced.

626 In the grid task, Pupil Labs often missed small corrective saccades (Figure 7). In the Free-Viewing
627 task, we observed longer fixation durations for the Pupil Labs glasses which readily can be explained by
628 missed small saccade amplitudes as well. Therefore, it is unsurprising that Pupil Labs also has problems
629 with detecting microsaccades, and in addition, similarly to the Free Viewing task, reports them as shorter
630 as our gold standard.

631 3.6 Results Task 5: Blink task

632 Blinks are often only detected to remove them when they are considered artifacts, but blinks can also be a
633 measure of interest. In this task, we asked participants to voluntarily blink after a short beep.

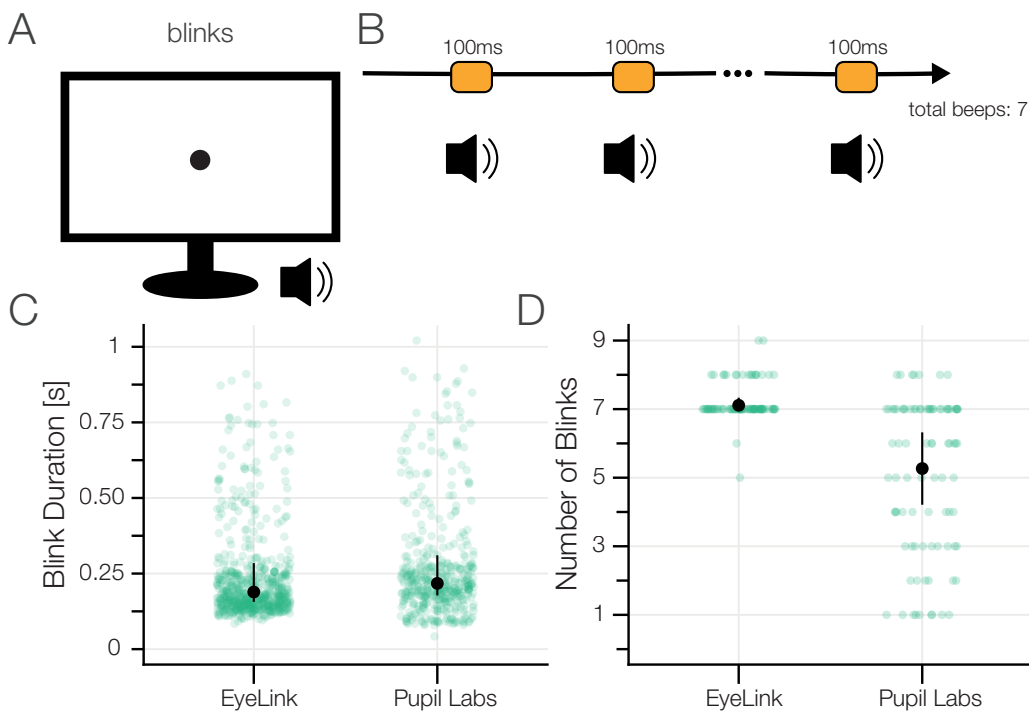


Figure 11. A) Blink task. B) The participants blinked after they heard a beep sound which was repeated 7 times. C) Blink durations. The eye-trackers' built-in blink detection algorithms were used. D) Number of detected blinks.

634 For EyeLink, the winsorized mean number of blinks was 7.1 (IQR: 7.0 to 7.33), for Pupil Labs 5.3
635 (IQR: 3.9 to 6.7), with a paired difference of 1.8 (CI_{95} : 3.1 to 0.8).

636 For EyeLink, the winsorized mean duration of a blink was 0.190 s (IQR: 0.154 s to 0.240 s), for Pupil
637 Labs 0.214 s (IQR: 0.170 s to 0.257 s), with a paired difference of -0.025 s (CI_{95} : -0.004 s to -0.039 s).

638 Typical voluntary blink duration is found to vary from 0.1 s to 0.4 s, with longer blinks reported from
639 Electrooculography (EOG) electrodes than by eye-trackers (VanderWerf et al., 2003; Benedetto et al.,

640 2011; Riggs et al., 1981; Lawson, 1948). EyeLink seems to find all seven blinks and some additional ones.
641 In contrast, Pupil Labs current blink detection algorithm is not sufficient to reliably detect eye blinks. We
642 even had to modify their blink detection algorithm (see Section 2.2.2) in order to use it in the first place.
643 Nevertheless, blinks were detected correctly for some subjects, but not on the group level.

644 3.7 Results Task 6: Pupil Dilation task

645 The pupil is constantly restricting and expanding mainly to accomodate for the amount of incoming light.
646 But many other influences have been found either from neurotransmitters, surprisal or during decision
647 making. We used 4 different luminance stimuli to measure the changing dilation of the participants'
648 pupils. Each luminance stimulus was preceded by a black baseline stimulus that was used to return pupil
649 to baseline size and the last second was used to normalize the measured pupil area.

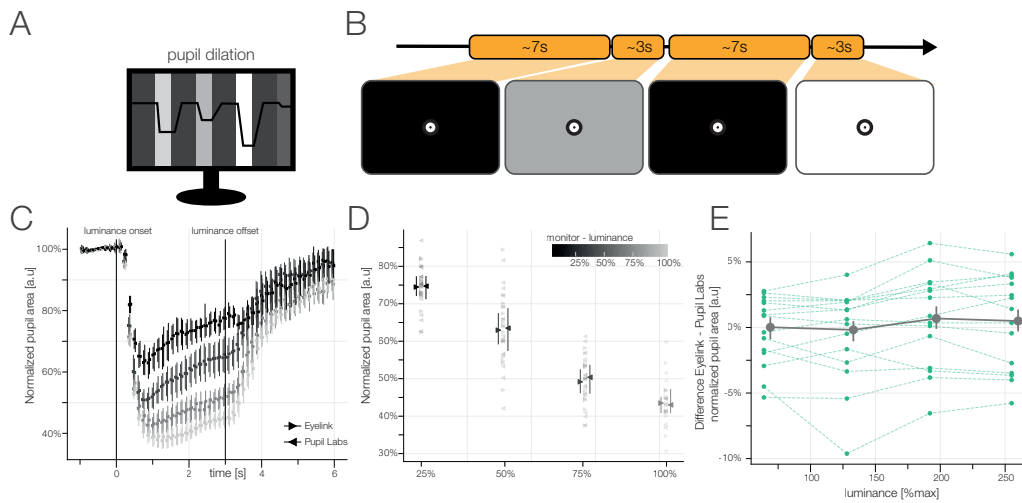


Figure 12. A) Pupil Dilation task. B) We showed participants 4 different luminance levels for 3 s each. Prior to each luminance, we showed a black baseline for 7 s. C) Change in normalized pupil area relative to median baseline for the 4 different luminance levels. Winsorized mean over participants of the winsorized means over blocks with 95% bootstrapped confidence intervals for each eye-tracker. D) Winsorized means and 95% bootstrapped confidence intervals of the pupil area for each luminance level. E) Difference in normalized pupil area between the eye-trackers. Each blue line refers to the winsorized mean of one luminance level of one participant. The aggregated data over subjects (gray line) illustrates that the measurements of the eye-trackers differ little on an aggregated level, but subject-wise the eye-trackers do estimate the size of the pupil area very differently.

650 On the group level, both eye-trackers seem to measure the same normalized pupil area (see Figure 12 C, D). However, looking at the estimates of pupil area per participant (Figure 12 E), we observe
651 that each of the eye-trackers has a reliable subject-specific bias. For some participants, EyeLink estimates
652 a consistently larger pupil than Pupil Labs. For other participants, it is the other way round. The difference
653 between eye-trackers of relative pupil size is constant per participant, even though the distance to the
654 maximal pupil size is not. That is, the eye-tracker difference at maximal constriction is the same as at the
655 maximal dilation. Because we look at relative pupil dilation, effectively the discrepancy per participant
656 between eye-tracker therefore increases with constricting pupil.

658 For this reason, researchers should be careful when relying on individual participants' pupil dilation.
659 However, on the group level, we think that there will be not much difference in using either eye-tracker.

660 3.8 Results Task 8/ Task 9: Head Movements

661 3.8.1 Results yaw movement

662 Eye movements rarely occur without head movements. In order to investigate eye movements in more
 663 natural paradigms, we need to know the influence of head movements on fixation accuracy. Therefore, we
 664 let participants move their head with their nose (and centered gaze) pointing to fixation targets presented
 665 on a horizontal line. In total we used 7 different target positions.

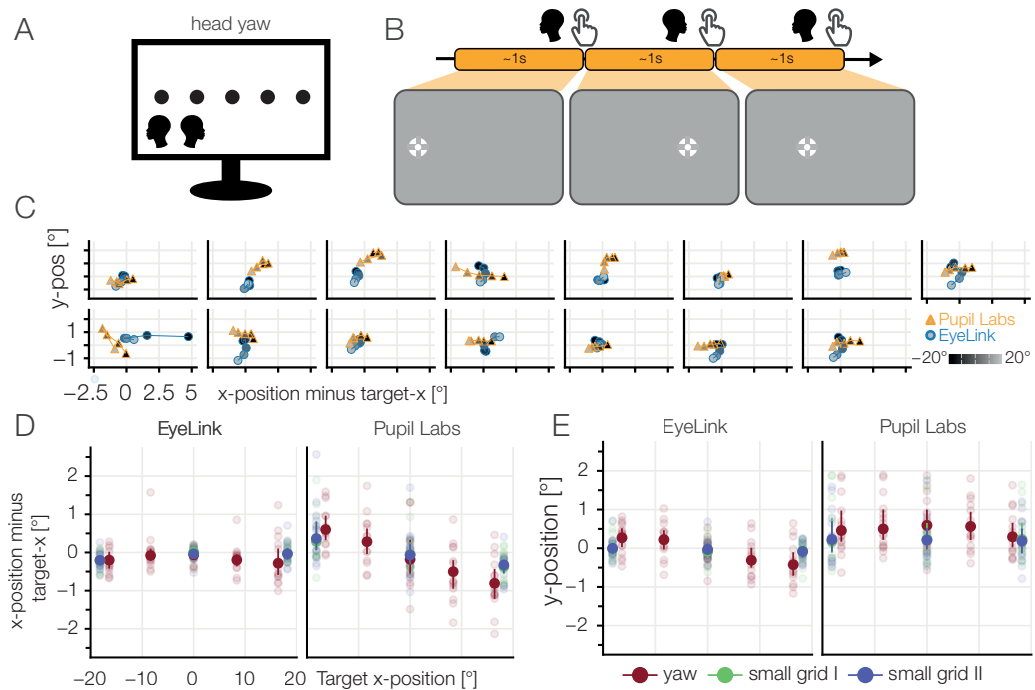


Figure 13. A) Head yaw task. B) The participants rotated their head so that their nose pointed to one of 5 horizontal targets. The participants pressed the space bar after they finished the head movement. C) Single subject plots: Distance of mean fixation to target fixation. An ideal fixation would cluster around (0,0). Constant offsets, as well as systematic drifts, can be found. Luminance indicates the position on the monitor (left: dark, right: bright). D) Deviation in horizontal gaze component (E) and vertical gaze component of the estimated gaze position to the target position (red). For comparison, results of small grid I & II are also included. The plots show the winsorized means over participants and blocks with a 95% confidence interval. Light points show the winsorized mean over the blocks for a single participant.

666 We observed that EyeLink estimated the horizontal component of the gaze relatively accurate, but the
 667 vertical component shows a systematic bias (compare Figure 13 D, E). The individual traces (Figure 13 C)
 668 show that half of the EyeLink participants show this pattern. Other participants are diffuse, either showing
 669 no effect of yaw movement or other idiosyncratic effects.

670 In contrast, Pupil Labs patterns are different. Here we find a systematic, larger effect in the horizontal
 671 component. In addition, the vertical gaze component shows a positive offset for all target positions. It
 672 could be possible that physical slippage of the glasses during the task or experiment due to head motion
 673 could be the reason for this offset in vertical accuracy. Both systematic biases can be found in reduced
 674 strength in the small grid conditions. Interestingly, the two small grid conditions, before and after the
 675 two head movement blocks, seem to be indistinguishable. This is a hint that the systematic effect we see
 676 during the yaw-task is a dependency on head position and not pure slippage.

677 **3.8.2 Results roll movement**

678 Similar to the head yaw, we also investigated head roll. We instructed the participants to roll their head
 679 until their eyes were aligned with a line that we presented at angles ranging from -15° to 15° . During the
 680 roll movement, the participants were instructed to keep their fixation on a central fixation target.

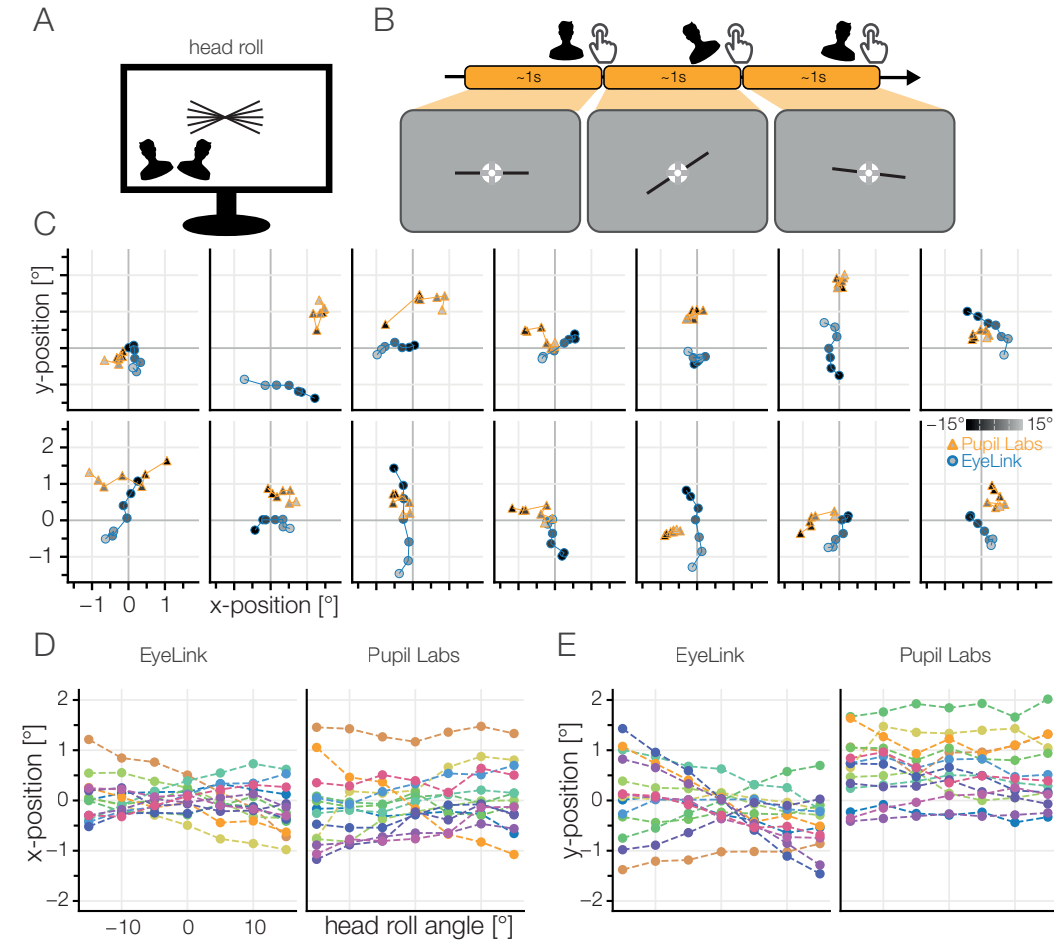


Figure 14. A) Head roll task. B) The participants tilted their head until their eyes were aligned with a skewed line and kept fixating a central fixation target. The skewed line was presented at 7 different angles from -15° to 15° . C) Individual participants' results. Mean fixation location is shown. In the ideal case, the points would be clustered around (0,0). Luminance indicates the position on the monitor (counterclockwise: dark, clockwise: bright). D) Deviation in horizontal gaze component or (E) vertical gaze component of the winsorized mean gaze position for all participants.

681 EyeLink shows a linear dependency of horizontal fixation position and head roll angle. The slope of
 682 this dependency differed between subjects from a negative slope to a slightly positive one. Interpreting the
 683 individual subject traces (Figure 14 C), it is clear that the vertical deviation is stronger in most participants.
 684 There seems to be no relation between the strengths of horizontal and vertical offset. For Pupil Labs, all
 685 slopes seem to be straight and we found only constant offsets. Conversely, in the individual participant
 686 traces Pupil Labs mostly shows a clustered but biased shape.

687 Both eye-trackers seem to have their own systematic problems with head movements. For traditional
 688 stationary experiments these biases can be ignored, for mobile setups with free head movements, these
 689 biases become much more important (cf. Niehorster et al., 2018). Taken together, we observed head
 690 movement biases of on average 1° for yaw and roll, with up to 3° in individual subjects. The resulting

691 biased accuracy values deviate to a great extend from the typical accuracy values that we observed in the
692 grid task.

693 4 DISCUSSION

694 4.1 Summary

695 In this paper, we recorded participants' gaze data using the EyeLink 1000 and the Pupil Labs glasses
696 simultaneously in a newly developed eye-tracking test battery. The gaze data was used to analyze a
697 multitude of eye-tracking related measures to compare the eye-trackers. Our test battery shows superior
698 accuracy as well as precision values for the EyeLink 1000 compared to the Pupil Labs glasses (average
699 accuracy: 0.57° vs. 0.82° ; average precision (SD): 0.19° vs. 0.31°). Similarly, we measured the decay
700 of calibration and the EyeLink 1000 was almost robust to this, while the Pupil Labs glasses showed a
701 decay by 30% after 4 min 30 s. Having a variety of eye-tracking tasks in our test battery, we also looked
702 at less typical performance measures. Our Free Viewing tasks allowed for more qualitative comparison
703 and indeed, we found large differences between the signals: Visual inspection showed high variance of
704 samples of the Pupil Labs glasses and quantitative analysis showed that the Pupil Labs glasses reported
705 fewer and shorter saccades and therefore also fewer fixations than the EyeLink. The effect of smaller
706 amplitudes is also reflected in other measures, e.g. a smaller rate of detected microsaccades. Our test
707 battery allows us to also look at the performance of blink detection and here we found accurate eye blink
708 detection by the Eyelink 1000 but not the Pupil Labs glasses. Looking at the impact of head movement on
709 the recorded gaze signals, we found that both eye-trackers were equally susceptible to head motion: the
710 EyeLink 1000 is more vulnerable to roll movements and the Pupil Labs glasses more to yaw movements.
711 We also observed that with both eye-trackers, pupil dilation seems to be recorded equally well on the
712 population level, but subject-wise, robust eye-tracker differences exist. Likewise, we did not find large
713 group differences between the eye-trackers in our model based task-specific smooth pursuit analysis.
714 This set of differences and similarities shows the importance of a heterogeneous test battery to compare
715 eye-trackers.

716 4.2 Accuracy

717 Accuracy is the dominant metric to evaluate eye-trackers, but as a single metric, it cannot summarize
718 performance for all typical eye-tracking experiments. Nevertheless, it is very useful and correlates
719 with many other evaluation metrics. We first discuss the results of the Eyelink 1000 followed by the
720 Pupil Labs Glasses.

721 Our measured winsorized mean accuracy for the EyeLink 1000 was 0.57° (which is larger than the
722 manufacturer-specified accuracy of $<0.5^\circ$). When comparing our measured value for the accuracy of the
723 EyeLink 1000 to values reported in the literature, we found comparable values from e.g. Barsingerhorn
724 (2018) who found mean accuracies of 0.56° horizontally and 0.73° vertically for the EyeLink 1000.
725 However, we also also encountered much worse accuracy values from Holmqvist (2017) who reports an
726 accuracy of $\approx 0.97^\circ$ for the EyeLink 1000 in a study comparing 12 eye trackers. Our measured accuracy
727 for the Pupil Labs glasses (0.82°) is larger than the manufacturer specified accuracy of 0.6° ($N = 8$,
728 Kassner et al., 2014) and very similar to a recent study comparing mobile eye-trackers ($N = 3$ MacInnes
729 et al., 2018) who reported 0.84° .

730 Given these accuracy results, researchers now can take consequences for their own studies. For
731 instance in a region of interest (ROI) analysis, they can make sure that their ROIs are much larger than
732 the eye-trackers fixation spread and accuracy. Holmqvist et al. (2012) offer such a simulation to test how
733 large the ROI needs to be, dependent on the precision of the eye-tracker. During the design of one's own
734 studies, one should perform these simulations and see for themselves if the paradigm, the size of ROI, or
735 if the device has to be changed.

736 Often researchers use a manufacturer calibration-validation procedure to get an estimate of the
737 accuracy. To validate such a procedure, we can compare the manufacturer values to our own results
738 (which were measured immediately after the manufacturer ones'): The EyeLink 1000 manufacturer
739 validation procedure accuracies were better than our own accuracy estimates (0.35° vs 0.57°). This is
740 surprising as the EyeLink 1000 software uses a similar procedure to our grid task (compare Section 2.3.4)
741 for their calibration/validation procedure (according to the SR-Support). It first detects saccades to find a
742 stable fixation and calculates the mean fixation position, then it calculates the Euclidean distance to the
743 validation target. While we make use of the spherical angle instead of Euclidean distance on the screen,

744 we do not think that this can explain such a large difference. Unfortunately, data from the manufacturer
745 validation procedure cannot be recorded simultaneously. Consequently, we currently do not know how
746 the deviation in accuracy values arises.

747 Interestingly, Pupil Labs' own validation procedure reported worse accuracies (1.04°) than what we
748 subsequently measured. In their case, this might be the result of their differing accuracy calculation
749 routine. Instead of selecting one fixation, they use every sample reported while the validation target
750 is visible. They then exclude samples too far from the target and the offset between the average of all
751 remaining samples to the displayed validation point are used to estimate the accuracy value. Hence, this
752 calculation results in a very conservative estimate as most likely some samples during the saccade or from
753 undershoot fixations are still included.

754 In summary, we found accuracy values that are worse than the manufacturer advertised ones, but
755 overall, the accuracy values were in a very good range for eye-tracking research.

756 **4.3 Results in the light of common experimental paradigms**

757 Our main motivation for this study was to determine that different experimental paradigms have different
758 requirements in regards to the eye-tracker performance. Thus there is not a single task that offers all data
759 to judge all task requirements. In a simple two-images choice paradigm, both tested eye-trackers are
760 equally suited to measure first fixation location and saccadic reaction time (e.g. Cludius et al., 2017) if the
761 images are large enough (usually such images are at least 5°). Switching to more natural tasks like free
762 viewing, one can see big differences between the eye-tracker in the quality of the signal of the individual
763 traces. While the aggregation in the Grid task shows good performance, visual inspection of the Free
764 Viewing task tells a different story. The Pupil Labs glasses exhibit much higher variance especially visible
765 during saccades. This makes the interpretation of single traces on free viewing paradigms difficult, but
766 aggregated measures (e.g. salience maps) should still be interpretable (Waechter et al., 2014).

767 Smooth pursuit eye movements are very common when moving through the world or watching
768 movies (or other dynamic stimuli). Our test battery tests smooth pursuit in a formal way and in this
769 paper we analyze smooth pursuit using a formal model as well. This is indebted due to the current lack
770 of applicable smooth pursuit detection algorithms (Pekkanen and Lappi, 2017; Bellet et al., 2018, but
771 see recent exceptions). We think that the smooth pursuit findings should be treated with caution as our
772 analysis might not generalize to more natural conditions and we had a high number of catch-up saccades.
773 Assuming they would indeed generalize, then both eye-trackers seem to be able to detect smooth pursuit
774 reliably.

775 If blink detection is important in an experiment, e.g. as a proxy for dopamine-related cognitive
776 functions (Riggs et al., 1981; but see Sescousse et al., 2018), then Pupil Labs should not be used, or a new
777 or custom blink detection algorithm has to be developed to detect blinks reliably.

778 Other experimental paradigms have even higher requirements: One class of examples are EEG/eye-
779 tracking combined studies which usually need very high temporal resolution to calculate fixation locked
780 signal averages (Dimigen et al., 2011; Ehinger et al., 2015), where even the small differences in fixation
781 onsets, which we found for Pupil Labs (see Figure 7 K), will result in a significant signal to noise ratio
782 reduction.

783 We were initially positively surprised on the performance of the Pupil Labs glasses to detect microsac-
784 cades. But quantitative analyses showed that only around 55% of gold-standard microsaccades were found.
785 Taken together with the qualitatively noisy main sequence it seems unlikely that more microsaccades can
786 be recovered by decreasing the microsaccade detection threshold of the algorithms or filtering the signal.
787 It might simply be, that the spatial precision of the Pupil Labs glasses is not high enough for microsaccade
788 studies.

789 For pupil dilation studies (e.g. Mathôt, 2018; Wahn et al., 2016) the eye-trackers do not seem to
790 differ on the group level. We investigated maximally large effects (black to white) and found reliable
791 non-additive differences for pupil dilation between the eye-trackers only on the individual subject's level.
792 But as most experiments are interested in the group-level, this finding should not pose a problem.

793 Head yaw, a very common head movement, posed a problem for both eye-trackers. The consequences
794 were not extreme, but notable ($\approx 1^\circ$ additional error for a large rotation of 40°). Head roll, which is less
795 common in mobile settings, had a systematic effect only on the remote EyeLink 1000 but not the Pupil
796 Labs glasses.

797 These interpretations are of course not exhaustive but show how such a diverse test battery allows to

798 evaluate eye-trackers on a task-individual basis. Consequently, this study allows researchers to plan and
799 select the eye-tracking equipment according to the design of their studies.

800 **4.4 Mobile settings**

801 As mentioned above, all of our results are based on data which were recorded under optimal lab conditions.
802 Therefore, we offer a lower bound for accuracy and only a rough basis for extrapolation to more mobile
803 setups. In realistic mobile setups, the calibration decay we observed will likely be worse as head
804 movements (and therefore slippage) increase. It is also possible that the 3D-eye algorithm offered by Pupil
805 Labs provides higher stability over time at the cost of overall worse accuracy, as it is advertised as no
806 slippage albeit on the cost of accuracy. This needs further testing. In general, there are many reasons that
807 make the analysis of mobile recordings more difficult: Firstly, the parallax error which occurs if one uses
808 a scene camera and fixations change in depth (Mardanbegi and Hansen, 2012; Narcizo and Hansen, 2015).
809 Secondly, due to uncontrolled pupil dilation changes (Brisson et al., 2013). Thirdly, head movements,
810 which we showed also in this experiment (Cesqui et al., 2013) and fourthly, due to large saccades to
811 eccentricities outside of the calibration range. This is by no means an exhaustive list, but just four reasons
812 as to why one will encounter difficulties when going into mobile settings. Further comparisons in mobile
813 settings and with mobile eye-trackers are needed (see a recent study with N=3 comparing three mobile
814 devices MacInnes et al., 2018).

815 **4.5 Eye-tracking test battery**

816 Our eye-tracking test battery proved to be reliable and exhaustive in this eye-tracking comparison study.
817 In case anyone would like to use the test battery to evaluate other eye-trackers, we recommend several
818 small changes in experimental design and analysis: 1) The smooth pursuit analysis should be based on an
819 analysis method that detects smooth pursuit without the prior information of smooth pursuit direction. We
820 tried to detect smooth pursuit directly and implemented the NSLR HMM algorithm (Pekkanen and Lappi,
821 2017) into our pipeline, which is one of the rare algorithms that offers smooth pursuit detection. But the
822 results were not usable for the Pupil Labs glasses, whereas the EyeLink 1000 was doing better (the bad
823 fusion of eyes could be one explanation, but we did not investigate further). We also found a very high
824 number of catch-up saccades even though following procedures described by a previous study. This needs
825 further investigation.

826 2) Some eye movement behaviors are missing from the test battery: e.g. vergence, calibration/validation
827 in depth and nystagmus. Especially for mobile setups (or VR-environments) calibration in depth would
828 be very interesting to evaluate.

829 3) A follow-up study should try to measure the true pupil size in addition to the one reported by the
830 eye-trackers. With this the individual subject differences we observed could be studied in greater detail.

831 In conclusion, it is clear that our eye-tracking test battery offers a extensive description of most eye
832 movement parameters and other missing parameters can easily be included in future versions.

833 **4.6 Pupil Labs: Ongoing development and Challenges**

834 The software and algorithms employed by Pupil Labs are continuously developed and improved. This
835 means that this comparison paper will always be outpaced by the new methodologies offered by Pupil
836 Labs and we can only test a snapshot of development. We want to point out that Pupil Labs offers the full
837 raw eye-videos, and any old analysis can, in principle, be updated with newer algorithms and software.
838 Our own analysis pipeline makes use of Pupil Labs' code and can be updated on demand. This is slightly
839 complicated by Pupil Labs, as they do not offer an official API, but one has to access the code of the
840 GUI-based software. Therefore, no guarantees for software compatibility over versions exist and our
841 pipeline (and those of other researchers) could break once Pupil Labs updates their algorithms. Therefore,
842 we recommend sticking to one recording and one analysis software version for the whole project. We also
843 want to note that the current GUI-based analysis software is easy for consumer use but quite difficult to
844 use for reproducible research. Using the GUI, many manual steps are necessary for each participant, to go
845 from eye-video recordings to accuracy values. Our own pipeline makes use of Pupil Labs' open source
846 code and circumvents these problems. To facilitate research with Pupil Labs, we offer our own makefile to
847 automatically compile most dependencies to run Pupil Labs from source, without the need for root-rights.

848 We noticed two problems with Pupil Labs' algorithms that could be directly improved upon. Blink
849 detection: Pupil Labs relies on the change in pupil-confidence (Section 2.2.2) instead of an absolute signal
850 (e.g. EyeLink uses a fixed number of frames without pupil detection). We had to improve their algorithms,

851 since we were often loosing large chunks of data (10's of seconds) to the failing blink detection algorithm.
852 Fusion of binocular recordings: We recorded binocularly, but often it seems that the reported trajectory
853 show eye-individual calibrations rather than binocular fusion (see Section 4 and Figure 9 C, D). Thus,
854 a high variance orthogonal to the saccade trajectory is introduced. The poor fusion of the eyes is also
855 reflected in the high standard deviation precision value. On one hand, this problem is likely influencing
856 velocity-based saccade detection algorithms like the one we used in this study. On the other hand, it is
857 unlikely that this problem influences the accuracy estimate, as we use fixation-wise mean gaze positions.
858 Another phenomenon related to bad fusion can be observed more in the temporal domain: While the
859 reported sampling frequency is 240 Hz, in practice, the effective sampling rate ranges from 120 Hz to
860 240 Hz (see Section 4). It is possible that future revisions of the software will fix these problems. In
861 the present study, the Pupil Labs eye-tracker served as a comparison to our gold standard. As to be
862 expected in such a comparison, both accuracy was worse and spatial precision smaller. Small saccades
863 were sometimes, blinks often, missed. But the average accuracy was well below 1° visual angle and pupil
864 dilation could be resolved as good as with our gold standard (as far as we can tell from our data). Thus,
865 taken together, it appears that the Pupil Labs eye-tracker is a valid choice when mid-range accuracy is
866 sufficient, repeated calibration is possible, medium-to-long saccades are to be expected and one does not
867 rely on the accurate detection of blinks.

868 **4.7 Limitations of the present study**

869 Our comparison study is limited, especially in how well it extrapolates to other situations. We used
870 only healthy, young, educated, western participants with 6/6 vision. And even from those we only
871 included $\approx 70\%$ in the study and rejected the others, as we could not calibrate them with both eye-trackers
872 concurrently. In a more diverse population, there are participant groups whose eye movements are
873 notoriously difficult to measure, for example children, elderly participants or some patients suffering from
874 autism (compare Barsingerhorn, 2018). The performance when measuring a less homogeneous population
875 remains to be measured, but will certainly be worse than our sample here. Therefore, we want to stress
876 again that our study reproduces a typical lab setup. In more advanced setups, e.g. mobile or VR studies,
877 the performance will also be worse due to more head movements.

878 Determining the detection algorithms used in the pipeline can have a general influence on the results.
879 In this study, we used a very popular velocity based saccade detector (Engbert and Mergenthaler, 2006).
880 This algorithm was developed for eye-trackers from SMI and SR-Research as the de-facto best video-
881 based eye-trackers for research. It is therefore possible that there is a bias against Pupil Labs when using
882 this algorithm. Pupil Labs offers their own fixation detector based on spatial dispersion, but informally
883 we found it lacking in many situations. The detection algorithm could have large effects on some of our
884 findings, e.g. precision, smooth pursuit speed, fixation number, and duration. However, we think that
885 the effect on spatial accuracy will be small. Indeed, using a new algorithm based on segmented linear
886 regression and a hidden markov model (Pekkanen and Lappi, 2017), we found near identical spatial
887 accuracy results, but the results for the precision measure and several others (e.g. the number and duration
888 of the fixations in the Free Viewing task) changed a lot. The comparison of algorithms is not the focus of
889 this article and has been done in other studies (Andersson et al., 2017).

890 There are more factors that might have given us non-optimal measured performances in our study:
891 The experimenter recording the data had less than a year of eye-tracking experience; we had to calibrate
892 two eye-trackers at the same time; and, at least for the EyeLink 1000, the calibration area on the monitor
893 was slightly larger than what is recommended (we used 36° with a recommended range of 32°). We argue
894 that these points cannot be critical, as we easily reached the manufacturer recommended validation results.
895 In addition, throughout the study we used robust statistics to mitigate the influence of singular outliers.

896 All in all, we think none of the limitations are so critical as to invalidate our findings.

897 **4.8 Conclusion**

898 Eye-tracking data quality cannot be reduced to a single value. Therefore we developed a new test battery
899 that allows to analyze a variety of eye-tracking measures. We used this test battery to evaluate two popular
900 eye-trackers and compare their performance. We exemplarily interpreted our findings in light of many
901 popular eye-tracking tasks and thereby offer guidance on how to interpret such results individually for the
902 researchers own tasks/eye-tracker combination.

903 **5 ACKNOWLEDGMENTS**

904 We thank Daniel Backhaus and Hans Trukenbrod for discussions, experimental code and stimulus material
905 for the free viewing task. We thank Anna and Ida Gert for valuable input throughout the project.

906 **6 CONFLICTS OF INTEREST:**

907 Peter König is the chief scientist of WhiteMatter Labs, an eye tracking related company. The Institute
908 of Cognitive Science owns seven Pupil Labs eye trackers and one Eyelink 1000. We are an independent
909 research group with no ties to the Pupil Labs company or to SR Research. We asked Pupil Labs for
910 recording recommendations and are still awaiting a reply (<https://github.com/pupil-labs/pupil/issues/1147>).
911

912 7 SUPPLEMENTARY MATERIALS

913 Comment Sheet

Table 1. Summary of participant information. *ELC failure* indicates a validation error consistently greater than 0.5° for the EyeLink 1000 during the initial calibration. Likewise, *PLC failure* indicates a validation error consistently greater than 1.5° for the Pupil Labs glasses. Only participants printed in bold font were included in the analysis.

Subject	Sex	Age	Dominant Eye	Handedness	Eye Color	Exclusion reason
1	f	27	right	right	blue green	-
2	f	24	left	right		-
3	f	21	right	right	blue	-
4	f	21	right	right	dark brown	-
5	f	20	left			PLC failure
6	f	25	right			Experiment crash
7	m	28	right	right	blue	PLC failure
8	f	22	left	right	dark brown	Experiment crash
9	f	25	right			Early Interrupt
10	f	26	right			PLC and ELC failure
11	m	24	left	right	light brown	-
12	m	21	right	right	light brown	-
13	f	25	left		blue green	ELC failure
14	f	24	right	right	blue	-
15	f	22	left	right	light brown	-
16	f	25	left	right	blue	ELC failure
17	f	27	right	right	dark brown	ELC failure
18	f	22	right			Experiment crash
19	m	29	right	right	dark brown	-
20	m	26	right	right	blue	-
21	m	23	left	right	blue	Recording Problems
22	m	28	right	right	blue	-
23	m	26	right	right	blue	-
24	f	25	right	right	blue	-
25	f	19	right	right	light brown	-
26	f	27	right	right	blue	-

914 REFERENCES

915 Andersson, R., Larsson, L., Holmqvist, K., Stridh, M., and Nyström, M. (2017). One algorithm to rule
916 them all? An evaluation and discussion of ten eye movement event-detection algorithms. *Behavior*
917 *Research Methods*, 49(2).

918 Açık, A., Sarvary, A., Schultze-Kraft, R., Onat, S., and König, P. (2010). Developmental Changes in
919 Natural Viewing Behavior: Bottom-Up and Top-Down Differences between Children, Young Adults
920 and Older Adults. *Frontiers in Psychology*, 1.

921 Backhaus, D. (2016). Mobiles Eye-Tracking Vergleichende Evaluation einer mobilen Eye-Tracking Brille.
922 Master's thesis, University of Potsdam.

923 Barsingerhorn, A. D. (2018). *Beyond visual acuity: Development of visual processing speed and*
924 *quantitative assessment of visual impairment in children*. PhD thesis, Radboud University Nijmegen.

925 Baumeister, A. A. and Joubert, C. E. (1969). Interactive effects on reaction time of preparatory interval
926 length and preparatory interval frequency. *Journal of Experimental Psychology*, 82(2).

927 Bellet, M. E., Bellet, J., Nienborg, H., Hafed, Z. M., and Berens, P. (2018). Human-level saccade detection
928 performance using deep neural networks. *Journal of Neurophysiology*.

929 Benedetto, S., Pedrotti, M., Minin, L., Baccino, T., Re, A., and Montanari, R. (2011). Driver workload
930 and eye blink duration. *Transportation Research Part F: Traffic Psychology and Behaviour*, 14(3).

931 Bonhage, C. E., Mueller, J. L., Friederici, A. D., and Fiebach, C. J. (2015a). Combined eye tracking
932 and fMRI reveals neural basis of linguistic predictions during sentence comprehension. *Special issue:*
933 *Prediction in speech and language processing*, 68.

934 Bonhage, C. E., Mueller, J. L., Friederici, A. D., and Fiebach, C. J. (2015b). Combined eye tracking
935 and fMRI reveals neural basis of linguistic predictions during sentence comprehension. *Special issue:*
936 *Prediction in speech and language processing*, 68.

937 Brainard, D. H. (1997). The Psychophysics Toolbox. *Spatial vision*, 10(4):433–436.

938 Brisson, J., Mainville, M., Mailloux, D., Beaulieu, C., Serres, J., and Sirois, S. (2013). Pupil diameter
939 measurement errors as a function of gaze direction in corneal reflection eyetrackers. *Behavior Research*
940 *Methods*, 45(4).

941 Burr, D. (2005). Vision: In the Blink of an Eye. *Current Biology*, 15(14).

942 Cesqui, B., de Langenberg, R. v., Lacquaniti, F., and d'Avella, A. (2013). A novel method for measuring
943 gaze orientation in space in unrestrained head conditions. *Journal of Vision*, 13(8).

944 Cludius, B., Wenzlaff, F., Briken, P., and Wittekind, C. E. (2017). Attentional biases of vigilance
945 and maintenance in obsessive-compulsive disorder: An eye-tracking study. *Journal of Obsessive-*
946 *Compulsive and Related Disorders*.

947 Cornelissen, F. W., Peters, E. M., and Palmer, J. (2002). The Eyelink Toolbox: eye tracking with MATLAB
948 and the Psychophysics Toolbox. *Behavior Research Methods, Instruments, & Computers*, 34(4).

949 Costela, F. M., Otero-Millan, J., McCamy, M. B., Macknik, S. L., Troncoso, X. G., Jazi, A. N., Crook,
950 S. M., and Martinez-Conde, S. (2014). Fixational eye movement correction of blink-induced gaze
951 position errors. *PloS one*, 9(10).

952 Dimigen, O., Sommer, W., Hohlfeld, A., Jacobs, A. M., and Kliegl, R. (2011). Coregistration of eye
953 movements and EEG in natural reading: analyses and review. *Journal of Experimental Psychology:*
954 *General*, 140(4).

955 Dowiasch, S., Marx, S., Einhäuser, W., and Bremmer, F. (2015). Effects of aging on eye movements in
956 the real world. *Frontiers in Human Neuroscience*, 9.

957 Duchowski, A. T. (2007). *Eye tracking methodology: theory and practice*. Springer, London.

958 Eckstein, M. K., Guerra-Carrillo, B., Miller Singley, A. T., and Bunge, S. A. (2017). Beyond eye gaze:
959 What else can eyetracking reveal about cognition and cognitive development? *Sensitive periods across*
960 *development*, 25.

961 Ehinger, B. V., König, P., and Ossandón, J. P. (2015). Predictions of Visual Content across Eye Movements
962 and Their Modulation by Inferred Information. *The Journal of Neuroscience*, 35(19).

963 Einhäuser, W. and König, P. (2010). Getting real—sensory processing of natural stimuli. *Sensory systems*,
964 20(3).

965 Einhäuser, W., Schumann, F., Bardins, S., Bartl, K., Böning, G., Schneider, E., and König, P. (2007).
966 Human eye-head co-ordination in natural exploration. *Network: Computation in Neural Systems*, 18(3).

967 Einhäuser, W., Schumann, F., Vockeroth, J., Bartl, K., Cerf, M., Harel, J., Schneider, E., and König, P.
968 (2009). Distinct Roles for Eye and Head Movements in Selecting Salient Image Parts during Natural

969 Exploration. *Annals of the New York Academy of Sciences*, 1164(1).

970 Engbert, R. and Kliegl, R. (2003). Microsaccades uncover the orientation of covert attention. *Vision
971 Research*, 43(9).

972 Engbert, R. and Mergenthaler, K. (2006). Microsaccades are triggered by low retinal image slip. *Proceed-
973 ings of the National Academy of Sciences*, 103(18).

974 Fischer, P., Ossandón, J. P., Keyser, J., Gulberti, A., Wilming, N., Hamel, W., Köppen, J., Buhmann, C.,
975 Westphal, M., Gerloff, C., Moll, C. K. E., Engel, A. K., and König, P. (2016). STN-DBS Reduces
976 Saccadic Hypometria but Not Visuospatial Bias in Parkinson's Disease Patients. *Frontiers in Behavioral
977 Neuroscience*, 10.

978 Holmqvist, K. (2017). Common predictors of accuracy, precision and data loss in 12 eye-trackers.

979 Holmqvist, K., Nyström, M., Andersson, R., Dewhurst, R., Jarodzka, H., and van de Weijer, J. (2011).
980 *Eye Tracking. A comprehensive guide to methods and measures*. Oxford University Press.

981 Holmqvist, K., Nyström, M., and Mulvey, F. (2012). Eye tracker data quality: what it is and how to
982 measure it. In *Proceedings of the Symposium on Eye Tracking Research and Applications*, Santa
983 Barbara, California. ACM.

984 Hunter, J. D. (2007). Matplotlib: A 2d Graphics Environment. *Computing in Science & Engineering*,
985 9(3).

986 Jones, E., Oliphant, T. E., Peterson, P., and others (2001). SciPy: Open source scientific tools for Python.

987 Kassner, M., Patera, W., and Bulling, A. (2014). Pupil: An Open Source Platform for Pervasive Eye
988 Tracking and Mobile Gaze-based Interaction. In *Adjunct Proceedings of the 2014 ACM International
989 Joint Conference on Pervasive and Ubiquitous Computing*, Seattle, Washington. ACM.

990 Kibirige, H., Lamp, G., Katins, J., O., A., gdowding, Funnell, T., matthias-k, Arnfred, J., Blanchard,
991 D., Chiang, E., Astanin, S., Kishimoto, P. N., Sheehan, E., Gibboni, R., Willers, B., stonebig, Pavel,
992 Halchenko, Y., smutch, zachcp, Collins, J., RK, M., Wickham, H., guoci, Brian, D., Arora, D., Brown,
993 D., Becker, D., Koopman, B., and Anthony (2018). has2k1/plotnine: v0.4.0. In *GitHub*.

994 Kleiner, M., Brainard, D., Pelli, D., Ingling, A., Murray, R., and Broussard, C. (2007). What's new in
995 Psychtoolbox-3. *Perception*, 36(14).

996 Knapen, T. (2016). hedfpy: convert SR Research eyelink edf output to tabular hdf5 format.

997 Koller, M. (2016). robustlmm : An R Package for Robust Estimation of Linear Mixed-Effects Models.
998 *Journal of statistical software*, 75.

999 Lawson, R. W. (1948). Photographic Evaluation of Blackout Indices. *Nature*, 162.

1000 Liston, D. B. and Stone, L. S. (2014). Oculometric assessment of dynamic visual processing. *Journal of
1001 Vision*, 14(14).

1002 Liversedge, S. P., Gilchrist, I., and Everling, S. (2012). *The Oxford Handbook of Eye Movements*. Oxford
1003 University Press.

1004 MacInnes, J. J., Iqbal, S., Pearson, J., and Johnson, E. N. (2018). Wearable Eye-tracking for Research:
1005 Automated dynamic gaze mapping and accuracy/precision comparisons across devices. *bioRxiv*.

1006 Mardanbegi, D. and Hansen, D. W. (2012). Parallax error in the monocular head-mounted eye trackers. In
1007 *Proceedings of the 2012 ACM Conference on Ubiquitous Computing*, Pittsburgh, Pennsylvania. ACM.

1008 Marius 't Hart, B., Vockeroth, J., Schumann, F., Bartl, K., Schneider, E., König, P., and Einhäuser, W.
1009 (2009). Gaze allocation in natural stimuli: Comparing free exploration to head-fixed viewing conditions.
1010 *Visual Cognition*, 17(6-7).

1011 Mathôt, S. (2018). Pupillometry: Psychology, Physiology, and Function. *Journal of Cognition*, 1(1).

1012 McKinney, W. (2010). Data Structures for Statistical Computing in Python. In *Proceedings of the 9th
1013 Python in Science Conference*.

1014 Mostert, P., Albers, A. M., Brinkman, L., Todorova, L., Kok, P., and de Lange, F. P. (2018). Eye Movement-
1015 Related Confounds in Neural Decoding of Visual Working Memory Representations. *eNeuro*, 5(4).

1016 Narcizo, F. B. and Hansen, D. W. (2015). Depth Compensation Model for Gaze Estimation in Sport
1017 Analysis. In *ICCV Workshops*.

1018 Niehorster, D. C., Cornelissen, T. H. W., Holmqvist, K., Hooge, I. T. C., and Hessels, R. S. (2018). What
1019 to expect from your remote eye-tracker when participants are unrestrained. *Behavior Research Methods*,
1020 50(1).

1021 Nyström, M., Hansen, D. W., Andersson, R., and Hooge, I. (2016). Why have microsaccades become
1022 larger? Investigating eye deformations and detection algorithms. *Fixational eye movements and
1023 perception*, 118.

1024 Oliphant, T. E. (2006). *A guide to NumPy*, volume 1. Trelgol Publishing, USA.

1025 Open Optometry (2018). Open Test Chart v4 Alpha: LogMar Test.

1026 Pekkanen, J. and Lappi, O. (2017). A new and general approach to signal denoising and eye movement
1027 classification based on segmented linear regression. *Scientific Reports*, 7(1).

1028 Pelli, D. G. (1997). The VideoToolbox software for visual psychophysics: transforming numbers into
1029 movies. *Spatial Vision*, 10(4).

1030 Petit, L., Clark, V. P., Ingeholm, J., and Haxby, J. V. (1997). Dissociation of Saccade-Related and Pursuit-
1031 Related Activation in Human Frontal Eye Fields as Revealed by fMRI. *Journal of Neurophysiology*,
1032 77(6).

1033 Plöchl, M., Ossandón, J., and König, P. (2012). Combining EEG and eye tracking: identification,
1034 characterization, and correction of eye movement artifacts in electroencephalographic data. *Frontiers
1035 in Human Neuroscience*, 6.

1036 Pupil Labs (2018). GitHub repository of pupil-labs/pupil. Version: f32ef8e.

1037 Riggs, L. A., Volkmann, F. C., and Moore, R. K. (1981). Suppression of the blackout due to blinks. *Vision
1038 Research*, 21(7).

1039 Rolfs, M. (2009). Microsaccades: Small steps on a long way. *Vision Research*, 49(20).

1040 Schumann, F., Einhäuser, W., Vockeroth, J., Bartl, K., Schneider, E., and König, P. (2008). Salient features
1041 in gaze-aligned recordings of human visual input during free exploration of natural environments.
1042 *Journal of Vision*, 8(14).

1043 Sescousse, G., Ligneul, R., van Holst, R. J., Janssen, L. K., de Boer, F., Janssen, M., Berry, A. S., Jagust,
1044 W. J., and Cools, R. (2018). Spontaneous eye blink rate and dopamine synthesis capacity: preliminary
1045 evidence for an absence of positive correlation. *European Journal of Neuroscience*, 47(9).

1046 Stoll, J., Chatelle, C., Carter, O., Koch, C., Laureys, S., and Einhäuser, W. (2013). Pupil responses allow
1047 communication in locked-in syndrome patients. *Current Biology*, 23(15).

1048 Tatler, B. W. (2007). The central fixation bias in scene viewing: Selecting an optimal viewing position
1049 independently of motor biases and image feature distributions. *Journal of Vision*, 7(14).

1050 Terhune, D. B., Sullivan, J. G., and Simola, J. M. (2016). Time dilates after spontaneous blinking. *Current
1051 Biology*, 26(11).

1052 Thaler, L., Schütz, A., Goodale, M., and Gegenfurtner, K. (2013). What is the best fixation target? The
1053 effect of target shape on stability of fixational eye movements. *Vision Research*, 76.

1054 Urai, A., Braun, A., and Donner, T. (2018). Pupil-linked arousal is driven by decision uncertainty and
1055 alters serial choice bias. *figshare*.

1056 van Rossum, G. (1995). Python tutorial, Technical Report CS-R9526. Technical report, Centrum voor
1057 Wiskunde en Informatica (CWI), Amsterdam.

1058 VanderWerf, F., Brassinga, P., Reits, D., Aramideh, M., and Ongerboer de Visser, B. (2003). Eyelid
1059 Movements: Behavioral Studies of Blinking in Humans Under Different Stimulus Conditions. *Journal
1060 of Neurophysiology*, 89(5).

1061 Waechter, S., Nelson, A. L., Wright, C., Hyatt, A., and Oakman, J. (2014). Measuring Attentional Bias to
1062 Threat: Reliability of Dot Probe and Eye Movement Indices. *Cognitive Therapy and Research*, 38(3).

1063 Wahn, B., Ferris, D. P., Hairston, W. D., and König, P. (2016). Pupil Sizes Scale with Attentional Load
1064 and Task Experience in a Multiple Object Tracking Task. *PLOS ONE*, 11(12).

1065 Wieser, M. J., Pauli, P., Alpers, G. W., and Mühlberger, A. (2009). Is eye to eye contact really threatening
1066 and avoided in social anxiety?—An eye-tracking and psychophysiology study. *Journal of Anxiety
1067 Disorders*, 23(1).

1068 Wilcox, R., editor (2012). *Introduction to Robust Estimation and Hypothesis Testing*. Academic Press,
1069 Boston.

1070 Wilmet, S. (2017). cosy-zeromq. Institute of NeuroSciences, Université Catholique de Louvain Belgium.

1071 Wilming, N. (2015). GitHub repository of pyedfread. Version: 3f3d7ad.

1072 Winterson, B. J. and Collewun, H. (1976). Microsaccades during finely guided visuomotor tasks. *Vision
1073 Research*, 16(12).

1074 Yuval-Greenberg, S., Tomer, O., Keren, A. S., Nelken, I., and Deouell, L. Y. (2008). Transient Induced
1075 Gamma-Band Response in EEG as a Manifestation of Miniature Saccades. *Neuron*, 58(3).